TABLE 4

Two-way analysis of variance results for GSTM1 and GSTT1 genotypes affecting remaining unchanged drug amounts of troglitazone and rosiglitazone

Source	Troglitazone			Rosiglitazone		
	Mean Square	*F*	*p*	Mean Square	*F*	*p*
GSTM1	242.6	8.25*	0.02	0.0	0.00	0.99
GSTT1	83.9	2.85	0.13	47.7	2.54	0.15
Interaction	0.1	0.00	0.96	20.9	1.11	0.32

* Significant at $p < 0.05$.

It was reported from an earlier clinical study that GSTM1 and GSTT1 null mutations might cause ALT and AST elevation by troglitazone (Watanabe et al., 2003). Therefore, we expected that low activity of detoxification enzymes, GSTs, may be risk factors. rhGSTT1 is not commercially available, but addition of rhGSTA1 or rhGSTM1 resulted in decreased microsomal CBLs of troglitazone and rosiglitazone (Fig. 2), suggesting that GSTA1 and GSTM1 potentially have a scavenger effect on reactive metabolites. Regarding the main GST isoforms, GSTA1 and GSTP1, null mutation or polymorphism-related clinical hepatotoxicity is unknown. Thus, although rhGSTA1 also potentially had the scavenger effect, CBLs of troglitazone and rosiglitazone in GSTM1- and GSTT1-genotyped hepatocytes were investigated (Fig. 3). Concentrations studied were determined by reference to the estimated unbound maximum concentration of troglitazone in the portal vein ($C_{in,\,max,\,u}$ = 1.4 μM; calculated in Supplemental 3). The concentrations of troglitazone and rosiglitazone were determined to be 10 μM to estimate an upper limit of hepatic exposure, and thus the concentration in this assay was considered to be reasonable for evaluation of hepatotoxicity. However, CBLs of troglitazone in GSTM1/GSTT1 null hepatocytes were significantly lower than those in GSTM1/GSTT1 wild-type hepatocytes (Fig. 3A; Table 3), independent of CYP3A or CYP2C8 activities (Fig. 3C). GSTs are well known to play crucial roles in detoxification of xenobiotics by preventing the binding of reactive metabolites to cellular proteins and catalyzing the conjugation of electrophilic moieties to GSH (Hayes et al., 2005). Our results were thus contrary to the expectation that GSTs would conjugate and decrease reactive metabolites and subsequent covalent binding, suggesting that microsomal CBL measurements with exogenous rhGSTM1 do not translate to the hepatocyte system with endogenous GSTM1. These are interesting findings because of the lack of CBL differences between GSTM1/GSTT1 null and wild-type hepatocytes with rosiglitazone (Fig. 3B;

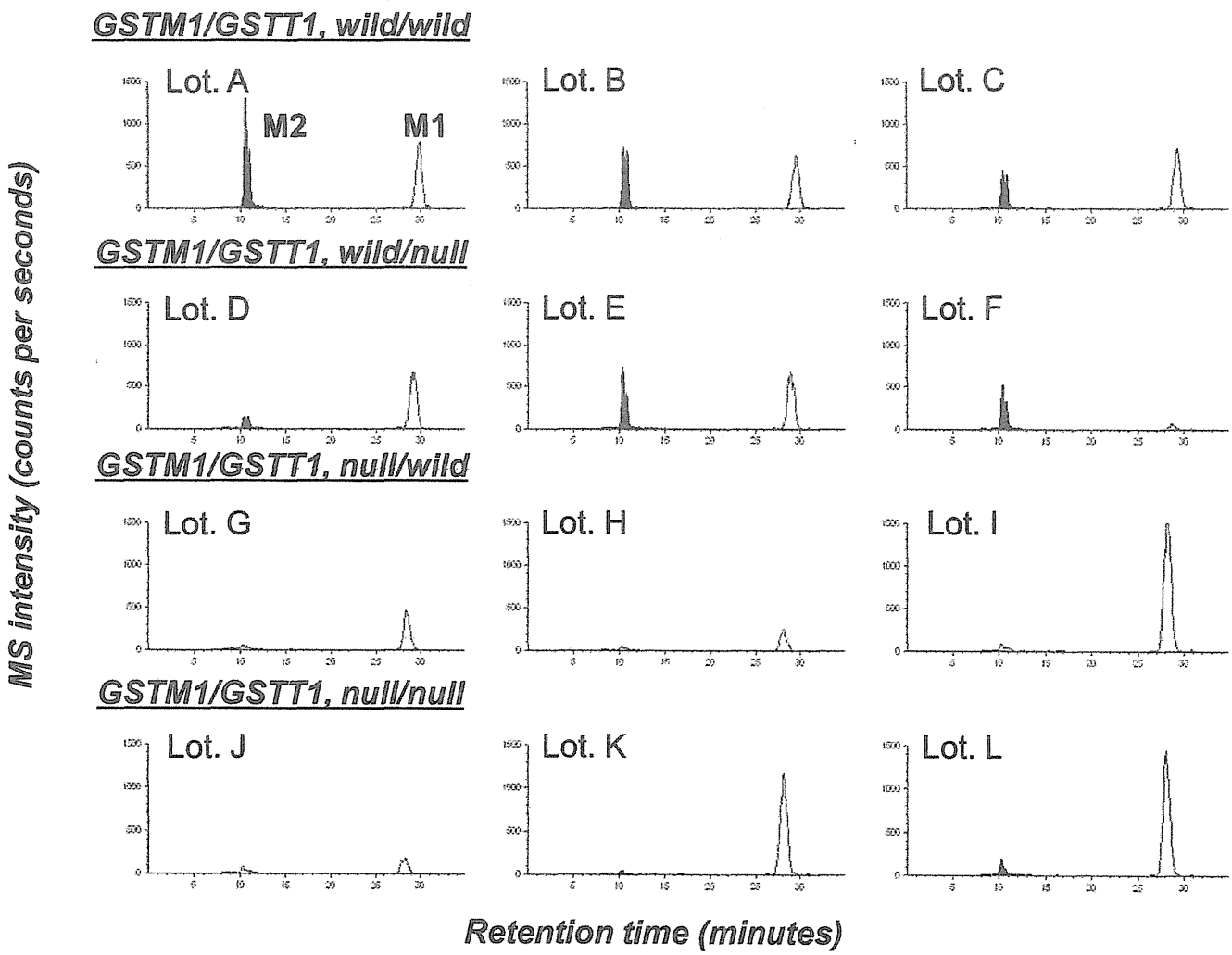

FIG. 5. LC-MS/MS chromatograms of troglitazone GSH adducts, M1 and M2, in GSTM1/GSTT1 null and wild-type hepatocytes. Filtrates after incubation of troglitazone (10 μM) with human hepatocytes genotyped for the GSTM1/GSTT1 null genotypes (lot A–C, wild/wild; lot D–F, wild/null; lot G–I, null/wild; and lot J–L, null/null) at 37°C for 8 h were applied to LC-MS/MS for detection of GSH adducts, M1 and M2, by means of the MRM method in the negative ion mode (MRM transitions: M1, $[M - H]^-$ = 745 → 272; M2, $[M - H]^-$ = 779 → 272).

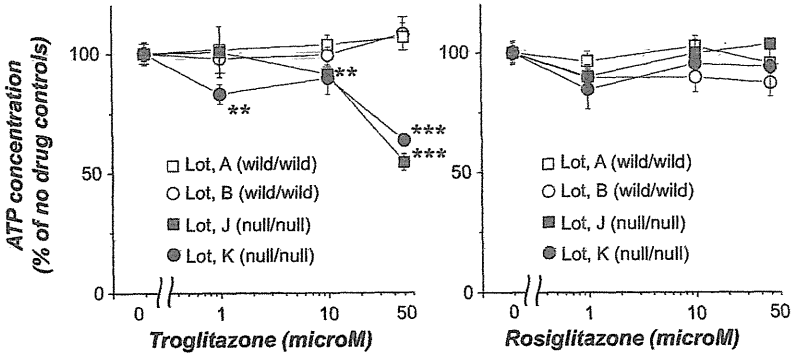

FIG. 6. Effects of GSTM1 and GSTT1 null mutations on cytotoxicity by troglitazone and rosiglitazone. Troglitazone and rosiglitazone were incubated with human cryopreserved hepatocytes genotyped for GSTM1/GSTT1 (□ and ○, wild/wild; ■ and ●, null/null) at 37°C for 2 h followed by measurement of ATP levels. Data are means ± S.D. from three assays expressed as percentages of the no drug control values. $p < 0.01$ was considered statistically significant. **, $p < 0.01$; ***, $p < 0.001$, significantly different from no drug controls.

Table 3), but unexplained, suggesting that not only CBL but also unknown factors are involved in the clinical outcomes of DILI.

In an attempt to clarify the discrepancy, metabolites of individual hepatocytes were analyzed by LC-MS/MS. Whereas M1 was found with all genotypes, M2 was scarcely obtained with GSTM1 null hepatocytes (Fig. 5). Because M2 formation is known to be catalyzed by CYP3A (Kassahun et al., 2001) and all hepatocytes used possessed a certain level of basal CYP3A activity (Table 2), it is reasonable to presume that GSTM1 is responsible for scavenging of a reactive metabolite trapped as M2. Verification of substrate selectivity for troglitazone-reactive metabolites trapped as M1 or M2 using rhGSTA1, rhGSTM1, and rhGSTP1 (Supplemental Fig. 2) indicated that M1 is formed by any GST isoforms but that M2 is formed only by rhGSTM1. It would therefore be possible to suggest that the GSH addition to a reactive metabolite to generate M1 might not be catalyzed by GSTM1, but a separate GSH addition to another metabolite to generate M2 could involve GSTM1 in hepatocytes. Specific exposure of GSTM1 null hepatocytes to the reactive metabolite trapped as M2 might have potential implications for understanding the relationship between troglitazone hepatotoxicity and GST genotypes in the clinical setting. The remaining unchanged troglitazone amounts in GSTM1 null hepatocytes were significantly higher than those in their GSTM1 wild-type counterparts (Fig. 4A; Table 4). Because troglitazone is known to be a time-dependent inhibitor of CYP3A (Kassahun et al., 2001), scavenging of reactive metabolites that bind to CYP3A protein by GSTM1 and maintaining the metabolic activity of troglitazone elimination could be a possible explanation for the discrepancy in CBL findings between exogenous rhGSTM1 and endogenous human GSTM1.

The cytotoxicity of troglitazone was investigated in the GSTM1- and GSTT1-genotyped hepatocytes. CYP3A and CYP2C8 activities affected reactive metabolite formation of troglitazone (Table 1). In addition, a combination of high CYP3A and UGT activities demonstrates association with low cytotoxicity of troglitazone, whereas low CYP3A with high SULT activity is linked to higher toxicity in human hepatocytes (Hewitt et al., 2002). However, ATP depletion was considered to be detected after treatment with troglitazone in GSTM1 and GSTT1 null hepatocytes specifically (Fig. 6) and independently of CYP2C8, CYP3A, UGT, and SULT activities (Table 2). This finding might be supportive evidence for GSTM1- and GSTT1-dependent hepatotoxicity in a clinical context, and this cytotoxicity would be expected to decrease the activities of reactive metabolite-forming enzymes and CBLs, providing another possible explanation for the discrepancy in CBL findings. Furthermore, it is interesting that GSTM1 and GSTT1 null mutation-dependent cytotoxicity was not observed for rosiglitazone.

Troglitazone sulfate, the main troglitazone metabolite eliminated into bile, shows competitive bile salt export pump inhibition with an apparent K_i value of 0.23 μM (Funk et al., 2001b). Treatment of GSTM1 and GSTT1 wild-type hepatocytes with 50 μM troglitazone did not reduce ATP levels, despite formation of a certain level of troglitazone sulfate (speculated from Supplemental Fig. 1B). Therefore, transporter inhibition might not be related to the cytotoxicity in the present study. By our system, however, the transporter activities were not investigated, and it remains to be determined whether clinical hepatotoxicity is caused by cytotoxicity or by transporter inhibition. Meanwhile, unchanged troglitazone has been reported to cause mitochondrial dysfunction (Masubuchi et al., 2006; Lim et al., 2008). Thus, our results cannot preclude the higher levels of unchanged drug in GSTM1/GSTT1 null hepatocytes (Fig. 4) being relevant to mitochondrial dysfunction. However, expression of CYP3A4 with γ-glutamylcysteine synthetase knockdown was shown to produce troglitazone cytotoxicity in a cell-based assay system (Hosomi et al., 2010, 2011), providing supportive information for our finding that high formation of reactive metabolites and low detoxification might be risk factors for troglitazone cytotoxicity.

At present, CBL is considered one of the most reliable tools to evaluate DILI (Evans et al., 2004; Nakayama et al., 2009; Usui et al., 2009). On the other hand, there are certainly some agents falsely identified as hepatotoxic by the CBL approach (Obach et al., 2008). In the case of troglitazone, CBLs of individual human hepatocytes phenotyped for P450s and genotyped for GSTs were not appropriate predictors for clinical hepatotoxicity, because the apparent inverse relationship for CBLs and cytotoxicity (and lack of P450 correlation) was observed in hepatocytes. Therefore, a cytotoxicity testing system using GSTM1- and GSTT1-genotyped hepatocytes may be more useful than a CBL measuring system using microsomes or hepatocytes. GSTM1/GSTT1 defects were found to relate to DILI with tacrine and carbamazepine in clinical studies (Simon et al., 2000; Ueda et al., 2007). It will now be necessary to investigate our evaluation system using GST-genotyped hepatocytes with more compounds.

In several recent studies, human leukocyte antigen (HLA) haplotypes were reported to be major determinants of DILI (e.g., flucloxacillin and lumiracoxib) (Daly et al., 2009; Singer et al., 2010), but the association between HLA haplotypes and troglitazone hepatotoxicity in the clinical context has not been reported. Because HLA haplotypes were not investigated in the present in vitro study, the immune idiosyncrasy in troglitazone cannot be precluded, and further study will be necessary.

In conclusion, our results demonstrate that GSTM1 and/or GSTT1 null mutations may cause higher exposure to the reactive metabolite trapped as M2 or direct cytotoxicity of troglitazone and appear to provide supportive evidence for metabolic idiosyncrasy of troglitazone hepatotoxicity in the clinical context. They are certainly informative for interpretation of mechanisms of troglitazone hepatotoxicity

and indicate that measurement of GSH adducts or cytotoxicity using GSTM1- and GSTT1-genotyped hepatocytes might offer an important in vitro system to assist in better prediction of DILI.

Acknowledgments

We acknowledge the contributions of Masashi Nakao and Dr. Tomoki Omodani in synthesizing radiolabeled compounds in-house. Appreciation is also expressed to Takeshi Takagaki for assistance with the statistical analyses and to Shinji Kimoto for assistance with the assays.

Authorship Contributions

Participated in research design: Usui, Hashizume, and Yokoi.

Conducted experiments: Usui.

Contributed new reagents or analytic tools: Usui.

Performed data analysis: Usui.

Wrote or contributed to the writing of the manuscript: Usui, Hashizume, Katsumata, Yokoi, and Komuro.

References

Arand M, Mühlbauer R, Hengstler J, Jäger E, Fuchs J, Winkler L, and Oesch F (1996) A multiplex polymerase chain reaction protocol for the simultaneous analysis of the glutathione S-transferase GSTM1 and GSTT1 polymorphisms. *Anal Biochem* **236:**184–186.

Bae MA and Song BJ (2003) Critical role of c-Jun N-terminal protein kinase activation in troglitazone-induced apoptosis of human HepG2 hepatoma cells. *Mol Pharmacol* **63:**401–408.

Daly AK, Donaldson PT, Bhatnagar P, Shen Y, Pe'er I, Floratos A, Daly MJ, Goldstein DB, John S, Nelson MR, et al. (2009) HLA-B*5701 genotype is a major determinant of drug-induced liver injury due to flucloxacillin. *Nat Genet* **41:**816–819.

Evans DC, Watt AP, Nicoll-Griffith DA, and Baillie TA (2004) Drug-protein adducts: an industry perspective on minimizing the potential for drug bioactivation in drug discovery and development. *Chem Res Toxicol* **17:**3–16.

Fujiwara T, Okuno A, Yoshioka S, and Horikoshi H (1995) Suppression of hepatic gluconeogenesis in long-term troglitazone treated diabetic KK and C57BL/KsJ-db/db mice. *Metabolism* **44:**486–490.

Funk C, Pantze M, Jehle L, Ponelle C, Scheuermann G, Lazendic M, and Gasser R (2001a) Troglitazone-induced intrahepatic cholestasis by an interference with the hepatobiliary export of bile acids in male and female rats. Correlation with the gender difference in troglitazone sulfate formation and the inhibition of the canalicular bile salt export pump (Bsep) by troglitazone and troglitazone sulfate. *Toxicology* **167:**83–98.

Funk C, Ponelle C, Scheuermann G, and Pantze M (2001b) Cholestatic potential of troglitazone as a possible factor contributing to troglitazone-induced hepatotoxicity: in vivo and in vitro interaction at the canalicular bile salt export pump (Bsep) in the rat. *Mol Pharmacol* **59:**627–635.

Gitlin N, Julie NL, Spurr CL, Lim KN, and Juarbe HM (1998) Two cases of severe clinical and histologic hepatotoxicity associated with troglitazone. *Ann Intern Med* **129:**36–38.

Hayes JD, Flanagan JU, and Jowsey IR (2005) Glutathione transferases. *Annu Rev Pharmacol Toxicol* **45:**51–88.

He K, Talaat RE, Pool WF, Reily MD, Reed JE, Bridges AJ, and Woolf TF (2004) Metabolic activation of troglitazone: identification of a reactive metabolite and mechanisms involved. *Drug Metab Dispos* **32:**639–646.

Hewitt NJ, Lloyd S, Hayden M, Butler R, Sakai Y, Springer R, Fackett A, and Li AP (2002) Correlation between troglitazone cytotoxicity and drug metabolic enzyme activities in cryopreserved human hepatocytes. *Chem Biol Interact* **142:**73–82.

Hosomi H, Akai S, Minami K, Yoshikawa Y, Fukami T, Nakajima M, and Yokoi T (2010) An in vitro drug-induced hepatotoxicity screening system using CYP3A4-expressing and γ-glutamylcysteine synthetase knockdown cells. *Toxicol In Vitro* **24:**1032–1038.

Hosomi H, Fukami T, Iwamura A, Nakajima M, and Yokoi T (2011) Development of a highly sensitive cytotoxicity assay system for CYP3A4-mediated metabolic activation. *Drug Metab Dispos* doi:10.1124/dmd.110.037077.

Isley WL (2003) Hepatotoxicity of thiazolidinediones. *Expert Opin Drug Saf* **2:**581–586.

Kassahun K, Pearson PG, Tang W, McIntosh I, Leung K, Elmore C, Dean D, Wang R, Doss G, and Baillie TA (2001) Studies on the metabolism of troglitazone to reactive intermediates *in vitro* and *in vivo*. Evidence for novel biotransformation pathways involving quinone methide formation and thiazolidinedione ring scission. *Chem Res Toxicol* **14:**62–70.

Lim PL, Liu J, Go ML, and Boelsterli UA (2008) The mitochondrial superoxide/thioredoxin-2/Ask1 signaling pathway is critically involved in troglitazone-induced cell injury to human hepatocytes. *Toxicol Sci* **101:**341–349.

Masubuchi Y, Kano S, and Horie T (2006) Mitochondrial permeability transition as a potential determinant of hepatotoxicity of antidiabetic thiazolidinediones. *Toxicology* **222:**233–239.

Nakayama S, Atsumi R, Takakusa H, Kobayashi Y, Kurihara A, Nagai Y, Nakai D, and Okazaki O (2009) A zone classification system for risk assessment of idiosyncratic drug toxicity using daily dose and covalent binding. *Drug Metab Dispos* **37:**1970–1977.

Nozawa T, Sugiura S, Nakajima M, Goto A, Yokoi T, Nezu J, Tsuji A, and Tamai I (2004) Involvement of organic anion transporting polypeptides in the transport of troglitazone sulfate: implications for understanding troglitazone hepatotoxicity. *Drug Metab Dispos* **32:**291–294.

Obach RS, Kalgutkar AS, Soglia JR, and Zhao SX (2008) Can in vitro metabolism-dependent covalent binding data in liver microsomes distinguish hepatotoxic from nonhepatotoxic drugs? An analysis of 18 drugs with consideration of intrinsic clearance and daily dose. *Chem Res Toxicol* **21:**1814–1822.

Russmann S, Jetter A, and Kullak-Ublick GA (2010) Pharmacogenetics of drug-induced liver injury. *Hepatology* **52:**748–761.

Saha S, New LS, Ho HK, Chui WK, and Chan EC (2010) Direct toxicity effects of sulfo-conjugated troglitazone on human hepatocytes. *Toxicol Lett* **195:**135–141.

Shiau CW, Yang CC, Kulp SK, Chen KF, Chen CS, Huang JW, and Chen CS (2005) Thiazolidenediones mediate apoptosis in prostate cancer cells in part through inhibition of Bcl-xL/Bcl-2 functions independently of PPARγ. *Cancer Res* **65:**1561–1569.

Shibuya A, Watanabe M, Fujita Y, Saigenji K, Kuwao S, Takahashi H, and Takeuchi H (1998) An autopsy case of troglitazone-induced fulminant hepatitis. *Diabetes Care* **21:**2140–2143.

Sigrist S, Bedoucha M, and Boelsterli UA (2000) Down-regulation by troglitazone of hepatic tumor necrosis factor-α and interleukin-6 mRNA expression in a murine model of non-insulin-dependent diabetes. *Biochem Pharmacol* **60:**67–75.

Simon T, Becquemont L, Mary-Krause M, de Waziers I, Beaune P, Funck-Brentano C, and Jaillon P (2000) Combined glutathione-S-transferase M1 and T1 genetic polymorphism and tacrine hepatotoxicity. *Clin Pharmacol Ther* **67:**432–437.

Singer JB, Lewitzky S, Leroy E, Yang F, Zhao X, Klickstein L, Wright TM, Meyer J, and Paulding CA (2010) A genome-wide study identifies HLA alleles associated with lumiracoxib-related liver injury. *Nat Genet* **42:**711–714.

Sparano N and Seaton TL (1998) Troglitazone in type II diabetes mellitus. *Pharmacotherapy* **18:**539–548.

Tettey JN, Maggs JL, Rapeport WG, Pirmohamed M, and Park BK (2001) Enzyme-induction dependent bioactivation of troglitazone and troglitazone quinone *in vivo*. *Chem Res Toxicol* **14:**965–974.

Ueda K, Ishitsu T, Seo T, Ueda N, Murata T, Hori M, and Nakagawa K (2007) Glutathione S-transferase M1 null genotype as a risk factor for carbamazepine-induced mild hepatotoxicity. *Pharmacogenomics* **8:**435–442.

Uetrecht J (2009) Immune-mediated adverse drug reactions. *Chem Res Toxicol* **22:**24–34.

Usui T, Mise M, Hashizume T, Yabuki M, and Komuro S (2009) Evaluation of the potential for drug-induced liver injury based on in vitro covalent binding to human liver proteins. *Drug Metab Dispos* **37:**2383–2392.

Walgren JL, Mitchell MD, and Thompson DC (2005) Role of metabolism in drug-induced idiosyncratic hepatotoxicity. *Crit Rev Toxicol* **35:**325–361.

Watanabe I, Tomita A, Shimizu M, Sugawara M, Yasumo H, Koishi R, Takahashi T, Miyoshi K, Nakamura K, Izumi T, et al. (2003) A study to survey susceptible genetic factors responsible for troglitazone-associated hepatotoxicity in Japanese patients with type 2 diabetes mellitus. *Clin Pharmacol Ther* **73:**435–455.

Watanabe T, Ohashi Y, Yasuda M, Takaoka M, Furukawa T, Yamato T, Sanbuissho A, and Manabe S (1999) Was it possible to predict liver dysfunction caused by troglitazone during the nonclinical safety studies? *Iyakuhin Kenkyu* **30:**537–546.

Yamamoto Y, Yamazaki H, Ikeda T, Watanabe T, Iwabuchi H, Nakajima M, and Yokoi T (2002) Formation of a novel quinone epoxide metabolite of troglitazone with cytotoxicity to HepG2 cells. *Drug Metab Dispos* **30:**155–160.

Address correspondence to: Toru Usui, Pharmacokinetics Research Laboratories, Dainippon Sumitomo Pharma Co., Ltd., 3-1-98, Kasugade-naka, Konohana-ku, Osaka, 554-0022, Japan. E-mail: toru-usui@ds-pharma.co.jp

Supplemental Material can be found at:
http://dmd.aspetjournals.org/content/suppl/2011/05/03/dmd.110.037077.DC1.html

0090-9556/11/3908-1388–1395$25.00
DRUG METABOLISM AND DISPOSITION
Copyright © 2011 by The American Society for Pharmacology and Experimental Therapeutics
DMD 39:1388–1395, 2011

Vol. 39, No. 8
37077/3701350
Printed in U.S.A.

Development of a Highly Sensitive Cytotoxicity Assay System for CYP3A4-Mediated Metabolic Activation[S]

Hiroko Hosomi, Tatsuki Fukami, Atsushi Iwamura, Miki Nakajima, and Tsuyoshi Yokoi

Drug Metabolism and Toxicology, Faculty of Pharmaceutical Sciences, Kanazawa University, Kakuma-machi, Kanazawa, Japan

Received November 4, 2010; accepted May 3, 2011

ABSTRACT:

Drug-induced hepatotoxicity, which is a rare but serious adverse reaction to a large number of pharmaceutical drugs, is sometimes associated with reactive metabolites produced by drug-metabolizing enzymes. In the present study, we constructed a cell-based system to evaluate the cytotoxicity of reactive metabolites produced by CYP3A4 using human hepatoma cells infected with an adenovirus vector expressing human CYP3A4 (AdCYP3A4). When seven hepatoma cell lines (HepG2, Hep3B, HLE, HLF, Huh6, Huh7, and Fa2N4 cells) were infected with AdCYP3A4, HepG2 cells showed the highest CYP3A4 protein expression and testosterone 6β-hydroxylase activity (670 pmol · min^{-1} · mg^{-1}). With the use of AdCYP3A4-infected HepG2 cells, the cytotoxicities of 23 drugs were evaluated by the 2-(2-methoxy-4-nitrophenyl)-3-(4-nitrophenyl)-5-(2,4-disulfophenyl)-2*H*-tetrazolium monosodium salt assay, and the cell viability when treated with 11 drugs (amiodarone, desipramine, felbamate, isoniazid, labetalol, leflunomide, nefazodone, nitrofurantoin, tacrine, terbinafine, and tolcapone) was significantly decreased. Moreover, the transfection of siRNA for nuclear factor erythroid 2-related factor 2 (Nrf2) to decrease the cellular expression level of Nrf2 exacerbated the cytotoxicity of some drugs (troglitazone, flutamide, acetaminophen, clozapine, terbinafine, and desipramine), suggesting that the genes regulated by Nrf2 are associated with the detoxification of the cytotoxicities mediated by CYP3A4. We constructed a highly sensitive cell-based system to detect the drug-induced cytotoxicity mediated by CYP3A4. This system would be beneficial in preclinical screening in drug development and increase our understanding of the drug-induced cytotoxicity associated with CYP3A4.

Introduction

Drug-induced hepatotoxicity is a rare but serious adverse reaction to a large number of pharmaceutical drugs (Boelsterli and Lim, 2007). One of the mechanisms suggested for the drug-induced hepatotoxicity is associated with reactive metabolites produced by drug-metabolizing enzymes (Guengerich and MacDonald, 2007). For example, if the reactive metabolites covalently bind to intracellular proteins, cellular dysfunctions are apparently produced, resulting in the loss of ionic gradients, a decline in ATP levels, actin disruption, cell swelling, and cell rupture (Beaune et al., 1987; Yun et al., 1993). Although drug-induced hepatotoxicity can be evaluated using laboratory animal models, species differences in drug-metabolizing enzymes or other factors between humans and laboratory animals have made the prediction of drug-induced cytotoxicity difficult. Several studies used human hepatocytes to evaluate the drug-induced cytotoxicity mediated by drug-metabolizing enzymes (Li et al., 1999; Gómez-Lechón et al., 2003), but this approach is often not applicable because of the poor availability of human liver, the high cost, the significant variability among human hepatocyte preparations, and, in particular, the unstable enzyme activities of human hepatocytes.

To date, several systems for evaluating drug-induced cytotoxicity mediated by drug-metabolizing enzymes have been developed. Yoshitomi et al. (2001) used HepG2 cells stably expressing human cytochrome P450 (P450) enzymes, and the viabilities of the cells expressing CYP1A2, CYP2E1, and CYP3A4 were decreased in an acetaminophen concentration-dependent manner. Vignati et al. (2005) demonstrated, using HepG2 cells transiently transfected with CYP3A4, that reactive metabolites of various hepatotoxic drugs such as albendazole, flutamide, and troglitazone were produced by CYP3A4. Our previous study showed that benzodiazepines such as flunitrazepam and nimetazepam were metabolically activated by CYP3A4 by coincubation with HepG2 cells and CYP3A4 Supersomes (Mizuno et al., 2009). Thus, several in vitro studies demonstrated that P450 enzymes, especially CYP3A4, are involved in the cytotoxicities of various kinds of drugs. However, transfection of P450 expression plasmids into cells generally could not achieve high expression of P450 enzymes. In addition, many studies used cells with GSH levels decreased by treatment with L-buthionine sulfoximine to easily detect the cytotoxicity. Indeed, the GSH-conjugating process is responsible for the detoxification of reactive metabolites, but we considered that cells with decreased nuclear factor erythroid 2-related

This work was supported by Health and Labor Science Research Grants from the Ministry of Health, Labor, and Welfare of Japan [Grant H20-BIO-G001].

Article, publication date, and citation information can be found at http://dmd.aspetjournals.org.

doi:10.1124/dmd.110.037077.

[S] The online version of this article (available at http://dmd.aspetjournals.org) contains supplemental material.

ABBREVIATIONS: P450, cytochrome P450; Nrf2, nuclear factor erythroid 2-related factor 2; GCLC, glutamate-cysteine ligase, catalytic subunit; GCLM, glutamate-cysteine ligase, modifier subunit; 3-HAA, 3-hydroxyacetanilide; RT, reverse transcription; PCR, polymerase chain reaction; GAPDH, glyceraldehyde-3-phosphate dehydrogenase; MOI, multiplicity of infection; WST-8, 2-(2-methoxy-4-nitrophenyl)-3-(4-nitrophenyl)-5-(2,4-disulfophenyl)-2*H*-tetrazolium monosodium salt; TBF-A, 7,7-dimethylhept-2-ene-4-ynal.

factor 2 (Nrf2) levels would also be useful to sensitively detect the cytotoxicity, because Nrf2 is a transcription factor that acts as a main regulator for the up-regulation of a group of genes coding antioxidant proteins and phase II drug-metabolizing enzymes, such as NADPH-quinone oxidoreductase 1, heme oxygenase-1, and glutamate-cysteine ligase, catalytic subunit (GCLC) and modifier subunit (GCLM) (Thimmulappa et al., 2002; Balogun et al., 2003; Nioi et al., 2003). In fact, it has been reported that Nrf2 knockout mice had increased susceptibility to acetaminophen (Chan et al., 2001).

In a previous study, we established an adenovirus that could overexpress human CYP3A4 (AdCYP3A4) (Hosomi et al., 2010). In this study, we developed a highly sensitive in vitro cell-based assay system using AdCYP3A4 and investigated whether CYP3A4 is involved in the cytotoxicity of 23 drugs that are known to cause hepatotoxicity in humans. In addition, we investigated whether treatment with siNrf2 exacerbates the drug-induced cytotoxicity mediated by CYP3A4.

Materials and Methods

Chemicals and Reagents. Acetaminophen, allopurinol, clozapine, corticosterone, cyclizine, dantrolene sodium, desipramine, disulfiram, erythromycin, felbamate, 3-hydroxyacetanilide (3-HAA), maprotiline, nefazodone, nilutamide, rosiglitazone, sulindac, tacrine, terbinafine, testosterone, tolcapone, troglitazone, and zafirlukast were obtained from Wako Pure Chemicals (Osaka, Japan). Flutamide, 6β-hydroxytestosterone, isoniazid, labetalol, and nitrofurantoin were obtained from Sigma-Aldrich (St. Louis, MO). Amiodarone and leflunomide were obtained from LKT Labs (St. Paul, MN) and Enzo Life Sciences, Inc. (Farmingdale, NY), respectively. ReverTra Ace (Moloney murine leukemia virus reverse transcriptase RNaseH Minus) was from Toyobo (Tokyo, Japan). The Adenovirus Expression Vector Kit (Dual Version), RNAiso, random hexamer, and SYBR Premix Ex Taq were obtained from Takara (Shiga, Japan). The QuickTiter Adenovirus Titer Immunoassay Kit was from Cell Biolabs (Tokyo, Japan). Stealth Select RNAi for Nrf2 (siNrf2) (accession number NM_006164) and Stealth RNAi Negative Control Medium GC Duplex #2 (siScramble), Lipofectamine RNAiMAX Reagent, and Lipofectamine 2000 were obtained from Invitrogen (Carlsbad, CA). Dulbecco's modified Eagle's medium was from Nissui Pharmaceutical (Tokyo, Japan). MFE support media (serum-free) was from MultiCell Technologies (Lincoln, RI). All primers were commercially synthesized at Hokkaido System Sciences (Sapporo, Japan). Other chemicals were of analytical or the highest grade commercially available.

Cell Culture. The 293 and HepG2 cells were obtained from American Type Culture Collection (Manassas, VA). The HLE and Huh7 cells were obtained from Japan Collection of Research Biosources (Tokyo, Japan) and RIKEN BioResource Center (Ibaraki, Japan), respectively. The Fa2N4 cells were obtained from MultiCell Technologies. The Hep3B, Huh6, and HLF cells were kindly provided by Dr. Shuichi Kaneko (Kanazawa University, Kanazawa, Japan). The 293, HepG2, Hep3B, HLE, HLF, Huh6, and Huh7 cells were maintained in Dulbecco's modified Eagle's medium containing 10% fetal bovine serum (Invitrogen), 3% glutamine, 16% sodium bicarbonate, and 0.1 mM nonessential amino acids (Invitrogen) in a 5% CO_2 atmosphere at 37°C. Fa2N4 cells were grown on collagen-coated flasks and maintained in MFE support media containing 10% fetal bovine serum. When adenovirus was used to infect the cell lines, a medium containing 5% fetal bovine serum was used.

siRNA Treatment. HepG2 cells were transfected with siNrf2 or siScramble by Lipofectamine RNAiMAX Reagent. According to the manufacturer's protocol, RNAi duplex-Lipofectamine RNAiMAX complexes were prepared and added to each well before the HepG2 cells were seeded (2.0×10^4 cells/well). The concentrations of siNrf2 and siScramble were 10 nM.

Total RNA Preparation from Hepatoma Cells and Real-Time RT-PCR. Total RNA from hepatoma cells was isolated using RNAiso. The RT procedure was described previously (Nakajima et al., 2006). Human Nrf2 was quantified by real-time RT-PCR using the Smart Cycler (Cepheid, Sunnyvale, CA). The sequences of sense and antisense primers were 5′-CAACACACGGTCCACAGC-3′ and 5′-CAATATTAAGACACTGTAACTC-3′, respectively. A 1-μl portion of the reverse-transcribed mixture was added to a PCR mixture containing 10 pmol of sense and antisense primers and 12.5 μl of SYBR Premix Ex Taq solution in a final volume of 25 μl. The PCR conditions were as follows: after an initial denaturation at 95°C for 30 s, the amplification was performed by denaturation at 94°C for 6 s and annealing and extension at 64°C for 20 s for 45 cycles. Human glyceraldehyde 3-phosphate dehydrogenase (GAPDH) mRNA was also quantified as described previously (Tsuchiya et al., 2004). The expression level of Nrf2 mRNA was normalized with the GAPDH mRNA level.

Nrf2 Protein Level. The Nrf2 protein level was measured as described previously (Nakamura et al., 2008) with slight modifications. Cell lysates (30 μg) were separated on 7.5% polyacrylamide gel electrophoresis and electrotransferred onto Immobilon-P polyvinylidene difluoride membrane (Millipore Corporation, Billerica, MA). The membranes were probed with polyclonal rabbit anti-Nrf2 antibody (H-300) (Santa Cruz Biotechnology, Inc., Santa Cruz, CA), polyclonal rabbit anti-human GAPDH polyclonal antibodies (Sekisui Medical, Tokyo, Japan), and anti-rabbit IgG-conjugated IRDye680, and an Odyssey infrared imaging system (LI-COR Biosciences, Lincoln, NE) were used for the detection. The relative expression level was quantified using ImageQuant TL Image Analysis software (GE Healthcare, Little Chalfont, Buckinghamshire, UK).

CYP3A4 Enzyme Activity. AdCYP3A4 was constructed in our previous study (Hosomi et al., 2010). HepG2 cells (3×10^5 cells/well) were seeded in 12-well plates. After a 24-h incubation, the cells were infected with AdCYP3A4 for 48 h at a multiplicity of infection (MOI) of 10 (MOI 10). Then, after a 1-h incubation with 100 μM testosterone, the concentration of 6β-hydroxytestosterone, a metabolite of testosterone by CYP3A4, in the medium was measured as described previously (Hosomi et al., 2010).

Cytotoxicity Assay. HepG2 cells (2.0×10^4 cells/well) were seeded in 96-well plates and, if necessary, were treated with siNrf2 or siScramble as described above. After a 24-h incubation, the cells were infected with AdCYP3A4 or the recombinant adenovirus vector expressing green fluorescence protein (AdGFP) constructed in our previous study (Hosomi et al., 2010). The titers of AdCYP3A4 and AdGFP were 6.4×10^8 and 2.1×10^8 plaque forming units/ml, respectively. Forty-eight hours after infection at MOI 10, the cells were treated with various drugs for 24 h. After incubation with the drugs, cell viability was quantified by 2-(2-methoxy-4-nitrophenyl)-3-(4-nitrophenyl)-5-(2,4-disulfophenyl)-2*H*-tetrazolium monosodium salt (WST-8) and ATP assays according to the manufacturer's protocol. The WST-8 assay, which is a modified 3-(4,5-dimethylthiazol-2-yl)2,5-diphenyl tetrazolium bromide assay, was performed using Cell Counting Kit-8 (Wako Pure Chemicals). After incubation with the drugs, Cell Counting Kit-8 reagent was added, and absorbance of WST-8 formazan was measured at 405 nm. The ATP assay was performed using a CellTiter-Glo Luminescent Cell Viability Assay (Promega, Madison, WI). After incubation with the drugs, CellTiter-Glo Reagent was added, and the generation of luminescent signals was recorded by using a 1420 ARVO MX luminometer (PerkinElmer Life and Analytical Sciences-Wallac Oy, Turku, Finland).

Statistical Analyses. Comparisons of two and several groups were made with a unpaired, two-tailed Student's *t* test and Dunnett's test, respectively. $P < 0.05$ was considered statistically significant.

Results

CYP3A4 Enzyme Activity in Various Hepatoma Cell Lines Infected with AdCYP3A4. To determine which hepatoma cell line is suitable for the evaluation of drug-induced cytotoxicity mediated by CYP3A4, seven hepatoma cell lines (HepG2, Hep3B, HLE, HLF, Huh6, Huh7, and Fa2N4 cells) were infected with AdCYP3A4 at MOI 10, and the testosterone 6β-hydroxylase activity was measured at a concentration of 100 μM (Fig. 1). Among these cell lines, HepG2 cells showed the highest enzyme activity (670 pmol · min^{-1} · mg $protein^{-1}$). Huh7 cells also showed moderate enzyme activity (233 pmol · min^{-1} · mg $protein^{-1}$), but the other cells showed activity at less than 100 pmol · min^{-1} · mg $protein^{-1}$. From this result, HepG2 cells were used in the subsequent studies.

Cytotoxic Effects of CYP3A4 on Cell Viability of HepG2 Cells. To investigate whether CYP3A4 is associated with the cytotoxicity of 23 drugs (acetaminophen, allopurinol, amiodarone, clozapine, cycliz-

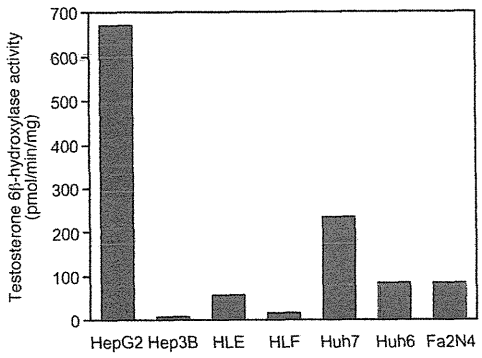

FIG. 1. CYP3A4 enzyme activity in various cell lines infected with AdCYP3A4. Cells were infected with AdCYP3A4 at MOI 10 for 48 h, and the testosterone 6β-hydroxylase activity was measured as described under *Materials and Methods*. Data are the means of two independent experiments.

ine, dantrolene, desipramine, disulfiram, erythromycin, felbamate, flutamide, isoniazid, labetalol, leflunomide, maprotiline, nefazodone, nitrofurantoin, sulindac, tacrine, terbinafine, tolcapone, troglitazone, and zafirlukast), HepG2 cells infected with AdCYP3A4 at MOI 10 for 48 h were treated with the drugs for 24 h (Fig. 2). As a negative control, AdGFP was infected at MOI 10. The cytotoxicity assay was performed at the concentrations less than the concentration that showed the typical decreased cell viability by the parent drugs. However, the range of concentrations was at least 30 times the clinically efficacious concentration or 100 μM according to a previous report (O'Brien et al., 2006). Cytotoxicity was evaluated by the WST-8 assay (Fig. 2), which showed that the viabilities of the cells infected with AdCYP3A4 were significantly decreased compared with that of those infected with AdGFP when treated with amiodarone (10 and 25 μM), desipramine (10 and 25 μM), disulfiram (25–100 μM), isoniazid (50 and 100 μM), leflunomide (100 μM), nefazodone (25 μM), tacrine (100 μM), terbinafine (10–50 μM), or tolcapone (20 and 50 μM). However, the other drugs did not affect the cell viability by the overexpression of CYP3A4 in the HepG2 cells.

Cytotoxic Effects of Knockdown of Nrf2 Expression on Cell Viability of HepG2 Cells. Nrf2 is a transcription factor that acts as an important regulator of the up-regulation of a group of genes coding antioxidant proteins and phase II drug-metabolizing enzymes, such as NADPH-quinone oxidoreductase, heme oxidase-1, and GCLC. Therefore, decreased Nrf2 levels in the cells may enhance the drug-induced cytotoxicity caused by CYP3A4. In this study, the drug-induced cytotoxicity mediated by CYP3A4 was investigated using AdCYP3A4-infected HepG2 cells transfected with siNrf2. The expression level of Nrf2 mRNA in HepG2 cells treated with siNrf2 for 72 and 96 h was lower than 90% of that of cells treated with siScramble (Fig. 3A). The expression level of Nrf2 protein in HepG2 cells treated with siNrf2 was also 55 to 75% lower than that of cells treated with siScramble (Fig. 3B). The effect of siNrf2 on the expression levels of Nrf2 mRNA and protein was not different between the treatments with AdGFP and AdCYP3A4. In addition, the HepG2 cell lysate treated with siNrf2 showed testosterone 6β-hydroxylase activity (781 ± 47 pmol · min^{-1} · mg $protein^{-1}$) similar to that of cell lysate treated with siScramble (720 ± 40 pmol · min^{-1} · mg $protein^{-1}$) (Fig. 3C). Therefore, it was confirmed that the decreased level of Nrf2 expression did not affect the testosterone 6β-hydroxylase activity.

With the use of HepG2 cells, the drug-induced cytotoxicity was investigated (Fig. 4). As a negative control against siNrf2, siScramble was transfected to HepG2 cells. Four drugs (troglitazone, flutamide, acetaminophen, and clozapine) that did not show cytotoxicity in the presence of CYP3A4 in the previous analysis (Fig. 2) and two drugs (desipramine and terbinafine) that showed cytotoxicity (Fig. 2) were investigated. In the WST-8 assay, the viabilities of AdCYP3A4-infected cells with siNrf2 were significantly decreased compared with those with siScramble for treatment with troglitazone (25 and 50 μM), flutamide (10–50 μM), acetaminophen (2.5–20 mM), clozapine (25–50 μM), desipramine (10 and 25 μM), or terbinafine (10 and 25 μM) (Fig. 4A). The ATP assay showed results similar to those of the WST-8 assay, although the magnitude of the difference in cell viability between cells with siNrf2 and those with siScramble was smaller (Fig. 4B). Thus, these results suggested that AdCYP3A4-infected HepG2 cells with decreased levels of Nrf2 were useful to evaluate the drug-induced cytotoxicity mediated by CYP3A4.

To investigate whether any drugs may affect the viability of cells with decreased levels of Nrf2, we examined the changes in cell viability by treatment with rosiglitazone, nilutamide, and 3-HAA, which have been reported to show a lower risk of hepatotoxicity but have structures similar to troglitazone, flutamide, and acetaminophen (Supplemental Fig. 1). However, rosiglitazone, nilutamide, and 3-HAA did not show decreased cell viability even when the Nrf2 level in cells was decreased. This result was consistent with the fact that these drugs are not likely to be associated with CYP3A4-mediated hepatotoxicity.

Discussion

Drug-induced hepatotoxicity is a rare but serious adverse reaction to a large number of pharmaceutical drugs (Boelsterli and Lim, 2007). Because drug-induced hepatotoxicity is sometimes associated with reactive metabolites produced by drug-metabolizing enzymes (Guengerich and MacDonald, 2007), it would be ideal to be able to predict the hepatotoxicity mediated by these enzymes using an in vitro system. In the present study, we constructed a highly sensitive cell-based system to detect the cytotoxicity of drugs using HepG2 cells expressing CYP3A4, which is a predominant P450 isoform in human liver that is responsible for more than 50% of drug metabolism (Guengerich, 2008).

In general, infection of cells with a recombinant adenovirus can lead to high expression of specific genes of interest. In our previous study, we introduced the overexpression of CYP3A4 protein in rat hepatoma cells, H4IIE cells, by the infection of AdCYP3A4 (Hosomi et al., 2010). Likewise, in this study, seven human hepatoma cell lines were infected with AdCYP3A4, and the testosterone 6β-hydroxylase activity was measured. Among them, HepG2 cells showed the highest enzyme activity (Fig. 1). This result might reflect the fact that HepG2 cells express high endogenous levels of NADPH-P450 reductase and cytochrome b_5 (Aoyama et al., 1990) in addition to the high efficiency of infection. The testosterone 6β-hydroxylase activity of AdCYP3A4-infected HepG2 cells (670 pmol · min^{-1} · mg $protein^{-1}$ at 100 μM testosterone) was more than 2.5-fold higher than the V_{max} values of the activity in human hepatocytes reported by Donato et al. (1995) and Gómez-Lechón et al. (2001) (177 ± 98 and 253 ± 110 pmol · min^{-1} · mg $protein^{-1}$, respectively). Given the large interindividual variability in CYP3A4 protein expression (a 32-fold variability) (Westlind-Johnsson et al., 2003), the cells used in this study would mimic human hepatocytes that exhibit the highest CYP3A4 enzyme activity.

In this study, we investigated the CYP3A4-mediated cytotoxicity of 23 drugs that are known to cause hepatotoxicity in humans (Xu et al., 2008). The viability of cells infected with AdCYP3A4 was significantly decreased by treatment with amiodarone, desipramine, disulfiram, isoniazid, leflunomide, nefazodone, nitrofurantoin, tacrine, terbinafine, and tolcapone compared with those infected with AdGFP. It has already been reported that the hepatotoxicity of some drugs is associated with the metabolic activation mediated by CYP3A4. The major metabolite of amiodarone, desethylamiodarone, was reported to

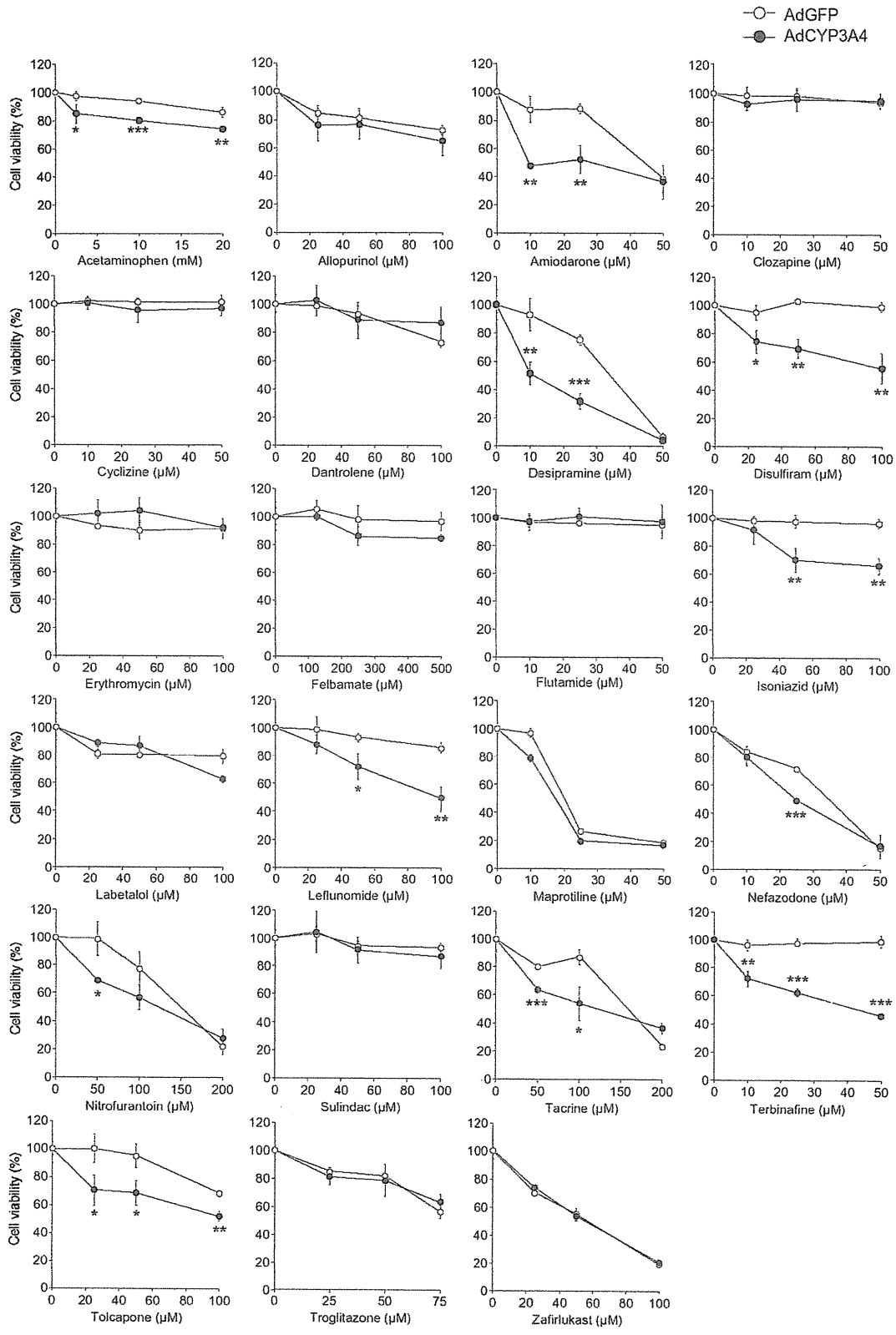

FIG. 2. Cytotoxic effects of CYP3A4 expression on cell viability of HepG2 cells treated with various drugs. HepG2 cells were infected with AdCYP3A4 (●) or AdGFP (○) at MOI 10 for 48 h and treated with 23 drugs for 24 h. Cell viability was measured by the WST-8 assay. Each point represents the mean ± S.D. ($n = 3$). *, $P < 0.05$; **, $P < 0.01$; ***, $P < 0.001$, compared with the AdGFP group at each concentration of the drug.

cause cytotoxicity in HepG2 cells and rat hepatocytes at lower concentrations than the parent drug amiodarone (McCarthy et al., 2004). Desethylamiodarone is produced mainly by CYP3A4 and by CYP2C8 in humans (Ohyama et al., 2000). Erythromycin-associated hepatic injury is usually cholestatic and may mimic obstructive jaundice (Klatskin, 1975). Although CYP3A4 is involved in erythromycin

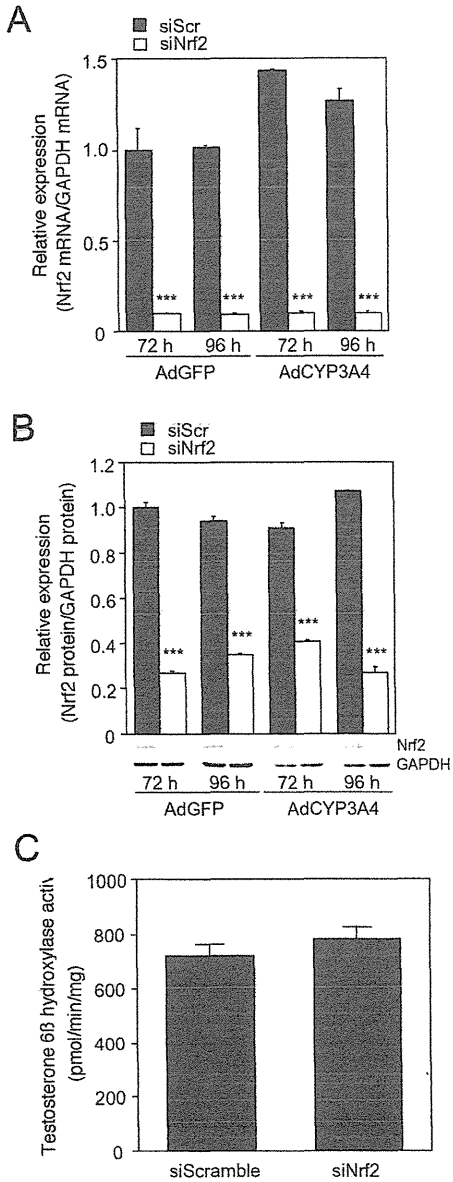

FIG. 3. Expression level of Nrf2 mRNA (A) and protein (B) and testosterone 6β-hydroxylase activity (C) in AdCYP3A4-infected HepG2 cells with siNrf2. After HepG2 cells were transfected with siNrf2 or siScramble at 10 nM followed by the infection with AdCYP3A4 or AdGFP at MOI 10 for 48 h, the expression level of Nrf2 mRNA and protein and testosterone 6β-hydroxylase activity were measured as described under *Materials and Methods*. Each column represents the means ± S.D. ($n = 3$). ***, $P < 0.001$ compared with AdCYP3A4-infected cells with siScramble.

metabolism and the substrate to which erythromycin binds has been identified (Watkins, 1992), it has no demonstrated relevance to erythromycin metabolism-associated hepatic injury. Nefazodone is metabolized to hydroxynefazodone, followed by the formation of quinone-imine and 2-chloro-1,4-benzoquinone, which would be associated with the hepatotoxicity, in human liver microsomes. These reactions are mediated by CYP3A4 (Kalgutkar et al., 2005). Terbinafine is mainly metabolized to *N*-demethylterbinafine, 7,7-dimethylhept-2-ene-4-ynal (TBF-A), and several hydroxy forms in human liver. Among them, TBF-A, which is produced by CYP3A4, was reported to cause terbinafine-induced hepatotoxicity (Iverson and Uetrecht, 2001). However, no association of CYP3A4 with desipramine-, disulfiram-, isoniazid-, leflunomide-, nitrofurantoin-, and tolcapone-induced hepatotoxicity has been reported, although most of these drugs appeared to be metabolically activated by P450 enzymes. For example, CYP1A2 is reported to be associated with the formation of iminoquinone from tacrine and tolcapone (Balson et al., 1995; Smith et al., 2003). Furthermore, CYP2E1 is considered to be associated with isoniazid-induced hepatotoxicity by metabolizing acetylhydrazine, one of the metabolites of isoniazid, to *N*-acetylhydrazine (Huang et al., 2003). Further studies on the involvement of CYP3A4 in the metabolic activation of these drugs are needed. Although pharmacological drug interactions were reported in cyclizine, a metabolic activation pathway would not be involved.

Nitroaromatic drugs such as tacrine and nitrofurantoin have been associated with liver injury (Boelsterli et al., 2006). In the reductive pathways from nitro to the fully reduced amine catalyzed mainly by cytochrome P450 reductase, several reactive metabolites including nitroso and *N*-hydroxylamine derivatives could be produced. The reductive metabolite of tacrine is produced by cytochrome P450 reductase in HepG2 cells, and the enhanced reactive oxygen species production results in cytotoxic effects (Osseni et al., 1999). Cytochrome P450 reductase is also involved in nitrofurantoin-induced redox cycling and cytotoxicity (Wang et al., 2008). There is no report suggesting the involvement of CYP3A4 in the metabolic activation of tacrine and nitrofurantoin. From these lines of evidence, the positive cytotoxic effects of tacrine and nitrofurantoin in Fig. 2 would be due to the cytochrome P450 reductase activity, which is highly expressed in tumor cells compared with hepatocytes. Flutamide is known to induce severe hepatic dysfunction. Ohbuchi et al. (2009) suggested that CYP3A4 catalyzed the N-oxidation of the amino metabolite of flutamide, which had hepatotoxic effects. Dantrolene was also implicated in the generation of reactive oxygen species via cytochrome P450 reductase. However, we previously reported that CYP3A4-mediated cytotoxicity was not involved in the effects of the nitroaromatic drugs, flutamide and dantrolene, which we investigated using CYP3A4-expressing rat BRL3A cells (Yoshikawa et al., 2009), supporting our present data in Fig. 2. Although the cytochrome P450 reductase-mediated redox reactions were suggested in flutamide- and dantrolene-induced hepatotoxicities, the underlying mechanism for metabolic activation is likely to be different for different drugs, producing different cytotoxic outcomes, an issue that needs to be clarified.

Felbamate induces the activity of CYP3A4, which accounts for the in vivo drug interactions in human (Glue et al., 1997). It was reported that felbamate heteroactivates the CYP3A4-mediated pathway (Egnell et al., 2003). However, these kinds of adverse effects were not detected in the present assay system, because only the cytotoxic effect by the CYP3A4-mediated metabolic activation of drug could be assessed. In addition, hepatotoxicity and hypersensitivity syndromes are associated with allopurinol (Al-Kawas et al., 1981; Arellano and Sacristán, 1993). Although the involvement of the CYP3A4-mediated reaction was still not clear, this kind of hepatotoxicity was also not detected in the present system.

A cytotoxic effect of metabolic activation of drug by CYP3A4 (Fig. 2, ●) was clearly demonstrated in a dose-dependent manner at 10 and 25 μM desipramine and nitrofurantoin. The cytotoxicity of parent drugs was demonstrated to be potent at 50 μM desipramine and nitrofurantoin and amiodarone (Fig. 2, ●). Thus, the effect of metabolic activation by CYP3A4 could not be detected at 50 μM concentrations of the drugs (Fig. 2), indicating that it should be considered the cytotoxicity of active metabolite(s) as well as that of the parent drugs at the various concentrations of drugs used in this in vitro assay system.

Nrf2 is the main regulator of the up-regulation of genes associated with detoxification reactions and is known to be constitutively and ubiquitously expressed in several tissues and cell lines. In the absence

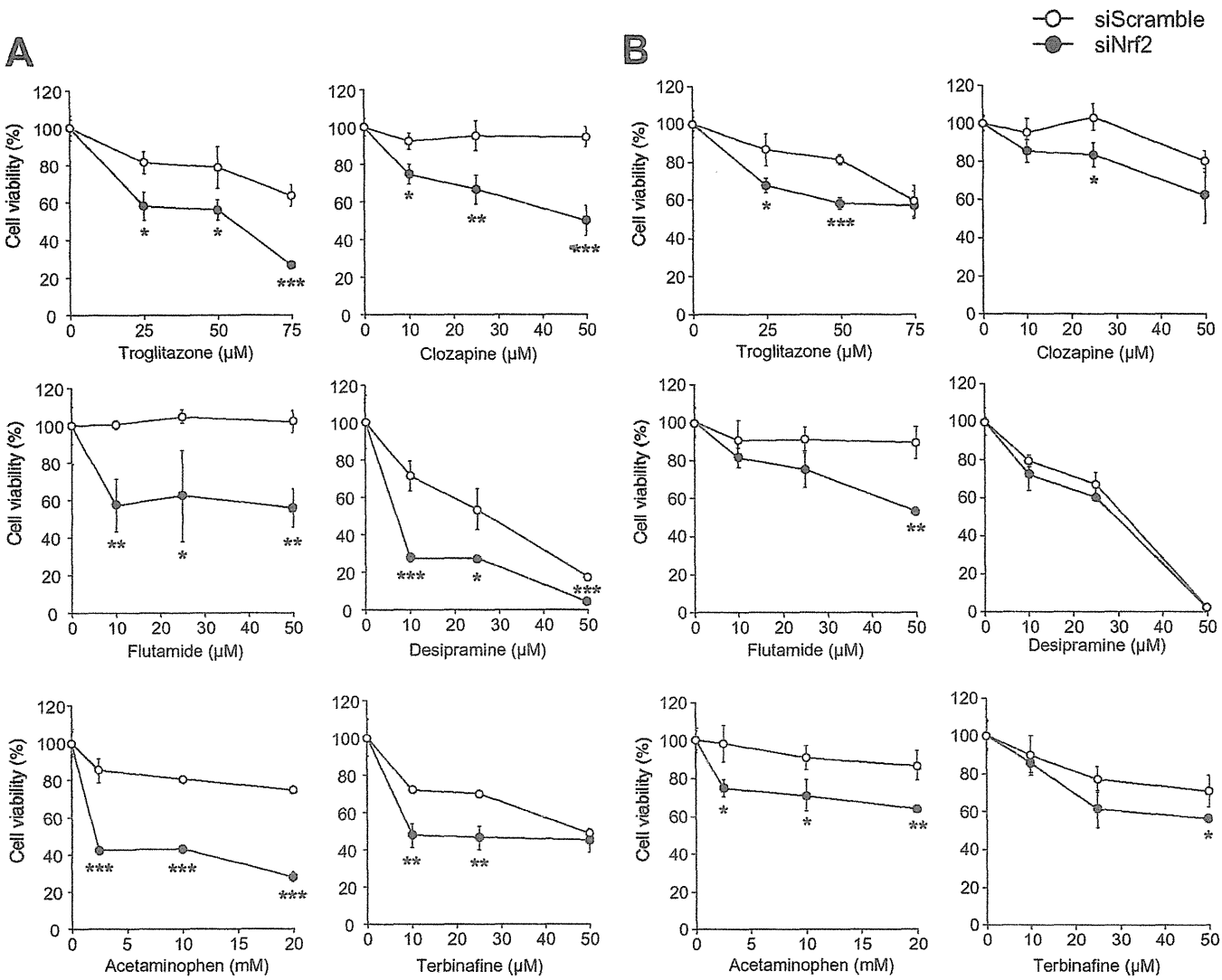

FIG. 4. Effects of the decreased level of Nrf2 on cell viability of CYP3A4-expressing HepG2 cells treated with the drugs. HepG2 cells were transfected with siNrf2 (●) or siScramble (○) at 10 nM for 24 h followed by infection with AdCYP3A4 at MOI 10 for 48 h. After cells were treated with six drugs for 24 h, WST-8 (A) and ATP (B) assays were performed for evaluation of the cell viability. Each point represents the mean ± S.D. ($n = 3$). *, $P < 0.05$; **, $P < 0.01$; ***, $P < 0.001$, compared with AdCYP3A4-infected cells with siScramble in each concentration of drug.

of cellular stress, Nrf2 is localized in the cytosol by binding with Kelch-like erythroid cell-derived protein with CNC homology-associated protein 1. When cells are exposed to oxidative stress, the newly synthesized Nrf2 accumulates in the nucleus (Kobayashi et al., 2006). However, it has been reported that Nrf2 is localized in the nucleus in HepG2 cells under nonstressed conditions (Nguyen et al., 2005). In the present study, HepG2 cells with decreased Nrf2 expression were used to detect the drug-induced cytotoxicity more sensitively. The Nrf2 mRNA level in HepG2 cells could be decreased to less than 10% by siNrf2 (Fig. 3A). Given that the Nrf2 mRNA level in HepG2 was 1.6-fold higher than that in human hepatocytes (data not shown), the HepG2 cells used in this study had approximately 20% of the Nrf2 mRNA expression as that in human hepatocytes.

The present study was conducted as shown in Fig. 4 with four drugs (troglitazone, flutamide, acetaminophen, and clozapine) that did not show cytotoxicity in AdCYP3A4-infected HepG2 cells without siNrf2 and two drugs that did show cytotoxicity (desipramine and terbinafine). The viabilities of cells transfected with siNrf2 were significantly decreased by treatment with the drugs compared with those transfected with siScramble (Fig. 4). These results suggest that the genes regulated by Nrf2 play important roles in the detoxification of the drug-induced cytotoxicities activated by CYP3A4. It has been reported that troglitazone is metabolized to quinone-type forms, which may be the reactive metabolites produced by CYP3A4 and CYP2C8 (Yamazaki et al., 1999). Although it has been reported that a postulated reactive metabolite of clozapine was produced by myeloperoxidase, leading to depletion of the cellular GSH level (Williams et al., 1997), there is no information about the association of CYP3A4 with the cytotoxicity of clozapine. Flutamide is reported be oxidized into reactive metabolites that covalently bind to microsomal proteins metabolized by CYP3A4 and CYP1A2 (Berson et al., 1993; Fau et al., 1994). In addition, acetaminophen is metabolized to *N*-acetyl-*p*-benzoquinone imine, a postulated ultimate reactive metabolite, by CYP2E1 and CYP3A4 in humans. These reactive metabolites could be trapped with GSH in a process that is the major detoxification pathway. Because GCLC, GCLM, and glutathione peroxidase, which are important factors for maintaining the cellular GSH level, are regulated by Nrf2 (Thimmulappa et al., 2002), the decreased viability of AdCYP3A4-infected cells with siNrf2 by these drugs may be due to the decreased level of cellular GSH. The reactive metabolite of

terbinafine, TBF-A, is known be trapped with GSH (Iverson and Uetrecht, 2001). The viability of AdCYP3A4-infected HepG2 cells was decreased by treatment with terbinafine even without siNrf2 transfection. This result was different from those by the treatment with troglitazone, flutamide, and acetaminophen. In addition, information about the association of CYP3A4/Nrf2 with desipramine-induced hepatotoxicity is limited, although epoxide formation and nitrosoalkane species were suggested to be related to the toxicity.

The WST-8 assay is a modified 3-(4,5-dimethylthiazol-2-yl)2,5-diphenyl tetrazolium bromide assay, a conventional cytotoxicity assay, that uses a highly water-soluble disulfonated tetrazolium salt as a chromogenic indicator. The WST-8 assay was used to measure the mitochondrial NADH enzymes as an indicator of cell viability. The ATP assay was used to measure the cellular concentration of ATP, which is produced in mitochondria. Thus, in both assays, the cell viability was evaluated by measuring the mitochondrial activity, but the sensitivity of the ATP assay is lower than that of the WST-8 assay (Fig. 4), and the result should therefore be carefully evaluated.

Many researchers have used cells transfected with P450 expression plasmids to investigate the drug-induced cytotoxicity mediated by P450s, but this system generally could not induce high expression of P450 enzymes. However, our established adenovirus-using system induced the overexpression of CYP3A4 in HepG2 cells, resulting in more than 2.5-fold higher enzyme activity than that of human hepatocytes. In addition, the transfection of siNrf2 to HepG2 cells could decrease to approximately 20% the Nrf2 expression level in human hepatocytes. Thus, the combination of AdCYP3A4 infection with the transfection of siNrf2 would enable sensitive detection of the drug-induced cytotoxicity mediated by CYP3A4.

In conclusion, we constructed a highly sensitive cell-based system to detect the drug-induced cytotoxicity mediated by CYP3A4. Furthermore, we found that a decrease in the level of Nrf2 could increase the sensitivity of detection for drug-induced cytotoxicity. It is generally known that very complicated mechanisms are involved in drug-induced liver injury and the basic mechanism is likely to be different for different drugs. Therefore, this in vitro assay system is not likely to predict in vivo drug-induced liver injury. However, this system would be beneficial in the preclinical screening in drug development and increase our understanding of the drug-induced cytotoxicity associated with CYP3A4.

Acknowledgments

We thank Brent Bell for reviewing the manuscript.

Authorship Contributions

Participated in research design: Hosomi, Fukami, Nakajima, and Yokoi.

Conducted experiments: Hosomi and Iwamura.

Performed data analysis: Hosomi, Fukami, and Iwamura.

Wrote or contributed to the writing of the manuscript: Hosomi, Fukami, and Yokoi.

References

Al-Kawas FH, Seeff LB, Berendson RA, Zimmerman HJ, and Ishak KG (1981) Allopurinol hepatotoxicity. Report of two cases and review of the literature. *Ann Intern Med* **95:**588–590.

Aoyama T, Korzekwa K, Nagata K, Gillette J, Gelboin HV, and Gonzalez FJ (1990) Estradiol metabolism by complementary deoxyribonucleic acid-expressed human cytochrome P450s. *Endocrinology* **126:**3101–3106.

Arellano F and Sacristán JA (1993) Allopurinol hypersensitivity syndrome: a review. *Ann Pharmacother* **27:**337–343.

Balogun E, Hoque M, Gong P, Killeen E, Green CJ, Foresti R, Alam J, and Motterlini R (2003) Curcumin activates the haem oxygenase-1 gene via regulation of Nrf2 and the antioxidant-responsive element. *Biochem J* **371:**887–895.

Balson R, Gibson PR, Ames D, and Bhathal PS (1995) Tacrine-induced hepatotoxicity. Tolerability and management. *CNS Drugs* **4:**168–181.

Beaune P, Dansette PM, Mansuy D, Kiffel L, Finck M, Amar C, Leroux JP, and Homberg JC (1987) Human anti-endoplasmic reticulum autoantibodies appearing in a drug-induced hepatitis are directed against a human liver cytochrome P-450 that hydroxylates the drug. *Proc Natl Acad Sci USA* **84:**551–555.

Berson A, Wolf C, Chachaty C, Fisch C, Fau D, Eugene D, Loeper J, Gauthier JC, Beaune P, and Pompon D (1993) Metabolic activation of the nitroaromatic antiandrogen flutamide by rat and human cytochromes P-450, including forms belonging to the 3A and 1A subfamilies. *J Pharmacol Exp Ther* **265:**366–372.

Boelsterli UA, Ho HK, Zhou S, and Leow KY (2006) Bioactivation and hepatotoxicity of nitroaromatic drugs. *Curr Drug Metab* **7:**715–727.

Boelsterli UA and Lim PL (2007) Mitochondrial abnormalities—a link to idiosyncratic drug hepatotoxicity? *Toxicol Appl Pharmacol* **220:**92–107.

Chan K, Han XD, and Kan YW (2001) An important function of Nrf2 in combating oxidative stress: detoxification of acetaminophen. *Proc Natl Acad Sci USA* **98:**4611–4616.

Donato MT, Castell JV, and Gómez-Lechón MJ (1995) Effect of model inducers on cytochrome P450 activities of human hepatocytes in primary culture. *Drug Metab Dispos* **23:**553–558.

Egnell AC, Houston B, and Boyer S (2003) In vivo CYP3A4 heteroactivation is a possible mechanism for the drug interaction between felbamate and carbamazepine. *J Pharmacol Exp Ther* **305:**1251–1262.

Fau D, Eugene D, Berson A, Letteron P, Fromenty B, Fisch C, and Pessayre D (1994) Toxicity of the antiandrogen flutamide in isolated rat hepatocytes. *J Pharmacol Exp Ther* **269:**954–962.

Gómez-Lechón MJ, Donato MT, Castell JV, and Jover R (2003) Human hepatocytes as a tool for studying toxicity and drug metabolism. *Curr Drug Metab* **4:**292–312.

Gómez-Lechón MJ, Donato T, Jover R, Rodriguez C, Ponsoda X, Glaise D, Castell JV, and Guguen-Guillouzo C (2001) Expression and induction of a large set of drug-metabolizing enzymes by the highly differentiated human hepatoma cell line BC2. *Eur J Biochem* **268:** 1448–1459.

Glue P, Banfield CR, Perhach JL, Mather GG, Racha JK, and Levy RH (1997) Pharmacokinetic interactions with felbamate. In vitro-in vivo correlation. *Clin Pharmacokinet* **33:**214–224.

Guengerich FP (2008) Cytochrome P450 and chemical toxicology. *Chem Res Toxicol* **21:**70–83.

Guengerich FP and MacDonald JS (2007) Applying mechanisms of chemical toxicity to predict drug safety. *Chem Res Toxicol* **20:**344–369.

Hosomi H, Akai S, Minami K, Yoshikawa Y, Fukami T, Nakajima M, and Yokoi T (2010) An in vitro drug-induced hepatotoxicity screening system using CYP3A4-expressing and γ-glutamylcysteine synthetase knockdown cells. *Toxicol in Vitro* **24:**1032–1038.

Huang YS, Chern HD, Su WJ, Wu JC, Chang SC, Chiang CH, Chang FY, and Lee SD (2003) Cytochrome P450 2E1 genotype and the susceptibility to antituberculosis drug-induced hepatitis. *Hepatology* **37:**924–930.

Iverson SL and Uetrecht JP (2001) Identification of a reactive metabolite of terbinafine: insights into terbinafine-induced hepatotoxicity. *Chem Res Toxicol* **14:**175–181.

Kalgutkar AS, Vaz AD, Lame ME, Henne KR, Soglia J, Zhao SX, Abramov YA, Lombardo F, Collin C, Hendsch ZS, et al. (2005) Bioactivation of the nontricyclic antidepressant nefazodone to a reactive quinone-imine species in human liver microsomes and recombinant cytochrome P450 3A4. *Drug Metab Dispos* **33:**243–253.

Klatskin G (1975) Toxic and drug-induced hepatitis, in *Diseases of the Liver*, 4th ed (Schiff L ed) pp 604–710, JB Lippincott, Philadelphia.

Kobayashi A, Kang MI, Watai Y, Tong KI, Shibata T, Uchida K, and Yamamoto M (2006) Oxidative and electrophilic stresses activate Nrf2 through inhibition of ubiquitination activity of Keap1. *Mol Cell Biol* **26:**221–229.

Li AP, Lu C, Brent JA, Pham C, Fackett A, Ruegg CE, and Silber PM (1999) Cryopreserved human hepatocytes: characterization of drug-metabolizing enzyme activities and applications in higher throughput screening assays for hepatotoxicity, metabolic stability, and drug-drug interaction potential. *Chem Biol Interact* **121:**17–35.

McCarthy TC, Pollak PT, Hanniman EA, and Sinal CJ (2004) Disruption of hepatic lipid homeostasis in mice after amiodarone treatment is associated with peroxisome proliferator-activated receptor-α target gene activation. *J Pharmacol Exp Ther* **311:**864–873.

Mizuno K, Katoh M, Okumura H, Nakagawa N, Negishi T, Hashizume T, Nakajima M, and Yokoi T (2009) Metabolic activation of benzodiazepines by CYP3A4. *Drug Metab Dispos* **37:**345–351.

Nakajima M, Itoh M, Sakai H, Fukami T, Katoh M, Yamazaki H, Kadlubar FF, Imaoka S, Funae Y, and Yokoi T (2006) CYP2A13 expressed in human bladder metabolically activates 4-aminobiphenyl. *Int J Cancer* **119:**2520–2526.

Nakamura A, Nakajima M, Higashi E, Yamanaka H, and Yokoi T (2008) Genetic polymorphisms in the 5′-flanking region of human UDP-glucuronosyltransferase 2B7 affect the Nrf2-dependent transcriptional regulation. *Pharmacogenet Genomics* **18:**709–720.

Nguyen T, Sherratt PJ, Nioi P, Yang CS, and Pickett CB (2005) Nrf2 controls constitutive and inducible expression of ARE-driven genes through a dynamic pathway involving nucleocytoplasmic shuttling by Keap 1. *J Biol Chem* **280:**32485–32492.

Nioi P, McMahon M, Itoh K, Yamamoto M, and Hayes JD (2003) Identification of a novel Nrf2-regulated antioxidant response element (ARE) in the mouse NAD(P)H:quinone oxidoreductase 1 gene: reassessment of the ARE consensus sequence. *Biochem J* **374:**337–348.

O'Brien PJ, Irwin W, Diaz D, Howard-Cofield E, Krejsa CM, Slaughter MR, Gao B, Kaludercic N, Angeline A, Bernardi P, et al. (2006) High concordance of drug-induced human hepatotoxicity with in vitro cytotoxicity measured in a novel cell-based model using high content screening. *Arch Toxicol* **80:**580–604.

Ohbuchi M, Miyata M, Nagai D, Shimada M, Yoshinari K, and Yamazoe Y (2009) Role of enzymatic N-hydroxylation and reduction in flutamide metabolite-induced liver toxicity. *Drug Metab Dispos* **37:**97–105.

Ohyama K, Nakajima M, Nakamura S, Shimada N, Yamazaki H, and Yokoi T (2000) A significant role of human cytochrome P450 2C8 in amiodarone N-deethylation: an approach to predict the contribution with relative activity factor. *Drug Metab Dispos* **28:**1303–1310.

Osseni RA, Debbasch C, Christen MO, Rat P, and Warnet JM (1999) Tacrine-induced reactive oxygen species in a human liver cell line: the role of anethole dithiolethione as a scavenger. *Toxicol In Vitro* **13:**683–688.

Smith KS, Smith PL, Heady TN, Trugman JM, Harman WD, and Macdonald TL (2003) In vitro metabolism of tolcapone to reactive intermediates: relevance to tolcapone liver toxicity. *Chem Res Toxicol* **16:**123–128.

Thimmulappa RK, Mai KH, Srisuma S, Kensler TW, Yamamoto M, and Biswal S (2002) Identification of Nrf2-regulated genes induced by the chemopreventive agent sulforaphane by oligonucleotide microarray. *Cancer Res* **62:**5196–5203.

Tsuchiya Y, Nakajima M, Kyo S, Kanaya T, Inoue M, and Yokoi T (2004) Human *CYP1B1* is regulated by estradiol via estrogen receptor. *Cancer Res* **64:**3119–3125.

Vignati L, Turlizzi E, Monaci S, Grossi P, Kanter R, and Monshouwer M (2005) An in vitro approach to detect metabolite toxicity due to CYP3A4-dependent bioactivation of xenobiotics. *Toxicology* **216:**154–167.

Wang Y, Gray JP, Mishin V, Heck DE, Laskin DL, and Laskin JD (2008) Role of cytochrome P450 reductase in nitrofurantoin-induced redox cycling and cytotoxicity. *Free Radic Biol Med* **44:**1169–1179.

Watkins PB (1992) Drug metabolism by cytochromes P450 in the liver and small bowel. *Gastroenterol Clin North Am* **21:**511–526.

Westlind-Johnsson A, Malmebo S, Johansson A, Otter C, Andersson TB, Johansson I, Edwards RJ, Boobis AR, and Ingelman-Sundberg M (2003) Comparative analysis of CYP3A expression in human liver suggests only a minor role for CYP3A5 in drug metabolism. *Drug Metab Dispos* **31:**755–761.

Williams DP, Pirmohamed M, Naisbitt DJ, Maggs JL, and Park BK (1997) Neutrophil cytotoxicity of the chemically reactive metabolite(s) of clozapine: possible role in agranulocytosis. *J Pharmacol Exp Ther* **283:**1375–1382.

Xu JJ, Henstock PV, Dunn MC, Smith AR, Chabot JR, and de Graaf D (2008) Cellular imaging predictions of clinical drug-induced liver injury. *Toxicol Sci* **105:**97–105.

Yamazaki H, Shibata A, Suzuki M, Nakajima M, Shimada N, Guengerich FP, and Yokoi T (1999) Oxidation of troglitazone to a quinone-type metabolite catalyzed by cytochrome P-450 2C8 and P-450 3A4 in human liver microsomes. *Drug Metab Dispos* **27:**1260–1266.

Yoshikawa Y, Hosomi H, Fukami T, Nakajima M, and Yokoi T (2009) Establishment of knockdown of superoxide dismutase 2 and expression of CYP3A4 cell system to evaluate drug-induced cytotoxicity. *Toxcol In Vitro* **23:**1179–1187.

Yoshitomi S, Ikemoto K, Takahashi J, Miki H, Namba M, and Asahi S (2001) Establishment of the transformants expressing human cytochrome P450 subtypes in HepG2, and their applications on drug metabolism and toxicology. *Toxicol In Vitro* **15:**245–256.

Yun CH, Okerholm RA, and Guengerich FP (1993) Oxidation of the antihistaminic drug terfenadine in human liver microsomes. Role of cytochrome P-450 3A(4) in N-dealkylation and C-hydroxylation. *Drug Metab Dispos* **21:**403–409.

Address correspondence to: Dr. Tsuyoshi Yokoi, Drug Metabolism and Toxicology, Faculty of Pharmaceutical Sciences, Kanazawa University, Kakuma-machi, Kanazawa 920-1192, Japan. E-mail: tyokoi@kenroku.kanazawa-u.ac.jp

0090-9556/11/3911-2057–2065$25.00
DRUG METABOLISM AND DISPOSITION
Vol. 39, No. 11
40907/3723773
Printed in U.S.A.

DMD 39:2057–2065, 2011

Progesterone Receptor Membrane Component 1 Modulates Human Cytochrome P450 Activities in an Isoform-Dependent Manner[S]

Shingo Oda, Miki Nakajima, Yasuyuki Toyoda, Tatsuki Fukami, and Tsuyoshi Yokoi

Drug Metabolism and Toxicology, Faculty of Pharmaceutical Sciences, Kanazawa, University, Kakuma-machi, Kanazawa, Japan

Received May 26, 2011; accepted August 8, 2011

ABSTRACT:

Cytochromes P450 (P450s) catalyze the metabolism of a wide spectrum of compounds. Recently, progesterone receptor membrane component 1 (PGRMC1), which shares a key structural motif with cytochrome b_5, has been reported to bind to sterol- or steroid-synthesizing P450s, enhancing their activities. In this study, we investigated whether PGRMC1 affects human drug-metabolizing P450 activities. Using coexpression systems for PGRMC1 and P450s (CYP3A4, CYP2C9, or CYP2E1) in HepG2 cells, we found that PGRMC1 decreased the V_{max} values and increased the K_m values of the CYP3A4 activities, and it decreased the V_{max} values but did not affect the K_m values of the CYP2C9 activities. In contrast, PGRMC1 hardly affected the CYP2E1 activities. These results suggest that PGRMC1 negatively modulates the drug-metabolizing activities of P450, although it was isoform but not substrate dependent. It is worth noting that coimmunoprecipitation analysis using coexpression systems for FLAG-PGRMC1 and Myc-P450s in human embryonic kidney 293 cells revealed that PGRMC1 interacts with all three P450s, although the affinity seemed to vary. In 29 human liver microsomes (HLMs), there was a 5-fold variability in the PGRMC1 protein levels. By the correlation analyses using the P450 activities and the PGRMC1 levels, we could neither observe the contribution of PGRMC1 to the P450 activities in HLMs nor that of the NADPH-cytochrome P450 reductase or cytochrome b_5. In conclusion, in contrast to sterol- or steroid-synthesizing P450s, we found that PGRMC1 negatively modulates the human drug-metabolizing activities of P450 through direct interaction. Further studies are needed to determine the clinical significance of PGRMC1 in the pharmacokinetics of drugs.

Introduction

Cytochrome P450 (P450) enzymes are heme-containing proteins that catalyze the metabolism of a wide variety of structurally diverse compounds (Nebert and Russell, 2002; Nelson et al., 2004). There are as many as 57 functional P450 genes and 58 pseudogenes in humans (http://drnelson.utmem.edu/CytochromeP450.html). Among them, three families, CYP1, CYP2, and CYP3, contribute to the oxidative metabolism of more than 70% of clinical drugs. Other P450 families (e.g., CYP4, CYP7, CYP11, CYP17, CYP19, CYP21, and CYP51) are involved in the metabolism of endogenous molecules such as steroids, bile acids, leukotrienes, and eicosanoids. P450 enzymes can exert their function by receiving electrons from NADPH-cytochrome P450 reductase (CPR) or cytochrome b_5 (Guengerich, 2002). CPR is indispensable for the P450 activities, whereas cytochrome b_5 has a significant role in the activities of some P450s (Shimada et al., 1994; Locuson et al., 2006).

Article, publication date, and citation information can be found at http://dmd.aspetjournals.org.
doi:10.1124/dmd.111.040907.
[S] The online version of this article (available at http://dmd.aspetjournals.org) contains supplemental material.

Progesterone receptor membrane component 1 (PGRMC1) was originally identified as a membrane-associated nongenomic receptor for progesterone (Cahill, 2007). Although it is predominantly localized in endoplasmic reticulum, it seems to be detected in the plasma membrane, nucleus, and cytoplasm (Cahill, 2007; Lösel et al., 2008). PGRMC1 is widespread in eukaryotes from yeast to human. Despite its name, it is controversial whether progesterone binds to PGRMC1 (Min et al., 2005; Peluso et al., 2008b), and its function has not been fully understood. PGRMC1 is expressed in many tissues including liver, kidney, brain, breast, and adrenals (Cahill, 2007; Lösel et al., 2008). PGRMC1, a 22-kDa protein, contains a transmembrane domain at the N-terminal and a cytochrome b_5-like domain to which heme binds in the middle (Mifsud and Bateman, 2002; Min et al., 2004, 2005; Ghosh et al., 2005). For the association of PGRMC1 with the P450 activities, there are several reports as follows. Laird et al. (1988) reported that monoclonal antibody to rat inner zone antigen, a synonym of PGRMC1, blocked the 21-hydroxylation of progesterone in rat adrenal tissue. Min et al. (2005) reported that coexpression of PGRMC1, but not that of a heme-deficient PGRMC1 mutant, enhanced the human CYP21A2 activity in COS-7 cells. Hughes et al. (2007) demonstrated that damage associated protein 1, the yeast homolog of PGRMC1, binds and positively regulates CYP51A1 and

ABBREVIATIONS: P450, cytochrome P450; Ad, adenovirus; CPR, NADPH-cytochrome P450 reductase; GFP, green fluorescent protein; HLM, human liver microsomes; HPLC, high-performance liquid chromatography; MOI, multiplicity of infection; PGRMC1, progesterone receptor membrane component 1; HEK, human embryonic kidney; PCR, polymerase chain reaction; HCM, hepatocyte culture medium; PAGE, polyacrylamide gel electrophoresis; siRNA, small interfering RNA.

CYP61A1, which catalyze sterol biosynthesis, and knockdown of endogenous PGRMC1 in human embryonic kidney (HEK) 293 cells resulted in the decreased cholesterol synthesis catalyzed by human CYP51A1. Thus, it has been demonstrated that PGRMC1 positively regulates P450-mediated sterol or steroid syntheses, making it "a helping hand for P450 proteins" (Debose-Boyd, 2007).

In contrast to endobiotic-metabolizing P450s, there is limited information on the effects of PGRMC1 on xenobiotic-metabolizing P450s. Although it was shown, by coimmunoprecipitation using a coexpression system in HEK293 cells, that PGRMC1 bound to CYP3A4 (Hughes et al., 2007), the functional significance remains to be clarified. In this study, we sought to investigate whether PGRMC1 might be a regulator of human drug-metabolizing P450 activities, focusing on CYP3A4, CYP2C9, and CYP2E1.

Materials and Methods

Chemicals and Reagents. Testosterone was purchased from Wako Pure Chemical Industries (Osaka, Japan). 7-Ethoxycoumarin, 7-hydroxycoumarin, chlorzoxazone, 6-hydroxychlrozoxazone, diclofenac, and *S*-warfarin were from Sigma-Aldrich (St. Louis, MO). 4′-Hydroxydiclofenac, 6β-hydroxytestosterone, and 7-hydroxywarfarin were purchased from BD Gentest (Woburn, MA), Steraloids (Newport, RI), and SAFC (St. Louis, MO), respectively. Midazolam and 1′-hydroxymidazolam were kindly provided by Astellas Pharmaceutical (Tokyo, Japan). Clonazepam was kindly provided by Roche Diagnostics (Basel, Switzerland). $NADP^+$, glucose 6-phosphate, and glucose-6-phosphate dehydrogenase were from Oriental Yeast (Tokyo, Japan). The Adenovirus Expression Vector kit (Dual Version) and QuickTiter Adenovirus Titer Immunoassay kit were from Takara (Osaka, Japan) and Cell Biolabs (Tokyo, Japan), respectively. The pTARGET vector was purchased from Promega (Madison, WI). Lipofectamine 2000 was from Invitrogen (Carlsbad, CA). All primers were commercially synthesized at Hokkaido System Science (Sapporo, Japan). Rabbit anti-human CYP3A4 polyclonal antibody and rabbit anti-human CYP2C9 antibody were from BD Gentest. Goat anti-rat CYP2E1 polyclonal antibody was from Nosan (Yokohama, Japan). Rabbit anti-human PGRMC1 polyclonal antibody and mouse anti-FLAG monoclonal antibody (M2) were from Sigma-Aldrich. Rabbit anti-human/rat CPR antibody was from Millipore (Billerica, MA). Rabbit anti-cytochrome b_5 antibody and mouse anti-c-Myc monoclonal antibody (9E10) were from Santa Cruz Biotechnology, Inc. (Santa Cruz, CA). Alexa Fluor 680 donkey anti-goat IgG was from Invitrogen. IRDye 680 goat anti-rabbit IgG and goat anti-mouse IgG were from LI-COR Biosciences (Lincoln, NE). All other chemicals and solvents were of the highest grade commercially available.

Construction of Recombinant Adenoviruses and Plasmids. Recombinant adenoviruses expressing CYP3A4 (AdCYP3A4), CYP2C9 (AdCYP2C9), and green fluorescent protein (AdGFP) were constructed as in our previous studies (Hosomi et al., 2010; Iwamura et al., 2011). Recombinant adenoviruses expressing PGRMC1 (AdPGRMC1) and CYP2E1 (AdCYP2E1) were created as follows. A fragment containing the full-length coding region of the human PGRMC1 or CYP2E1 cDNA was amplified by PCR using the primer pairs shown in Table 1 with a human liver cDNA as a template. The fragments were subcloned into the pAxCAwtit vector at a SwaI site. These vectors and the adenovirus genome DNA-terminal protein complex were cotransfected into HEK293 cells by Lipofectamine 2000. The recombinant adenovirus was isolated and propagated. Viral titers were determined using the QuickTiter Adenovirus Titer Immunoassay kit. The multiplicity of infection (MOI) was defined as the ratio of infectious units divided by the number of cells.

Expression vector for human PGRMC1 containing FLAG tag at the C terminus (FLAG-PGRMC1) was constructed as follows. Human PGRMC1 cDNA was amplified by PCR using the primers S-PGRMC1 and AS-FLAG PGRMC1 (Table 1) with the human liver cDNA as a template. The AS-FLAG PGRMC1 primer contains complementary sequences of FLAG tag and a stop codon. The PCR product was digested with BamHI and XhoI and ligated into the pcDNA3.1 Hygro+ vector (Invitrogen).

Expression vectors for human P450s (CYP3A4, CYP2C9, and CYP2E1) containing 3×Myc tag at the C terminus (Myc-P450) were constructed as follows. Once P450 cDNA lacking a stop codon was amplified by PCR with the primer pairs shown in Table 1, it was digested with XhoI and KpnI and subcloned into the pTARGET vector digested with the same restriction enzymes (pTARGET/P450 stop-). A double-strand DNA fragment containing three tandem copies of Myc tag sequence followed by a stop codon (Table 1) was subcloned into the pTARGET/P450 stop- plasmids digested with KpnI and NotI. The nucleotide sequences of the constructed plasmids were confirmed by DNA sequencing analyses.

Cell Cultures. Human embryonic kidney cell line HEK293 and human hepatocellular carcinoma cell line HepG2 were obtained from American Type Culture Collection (Manassas, VA) and Riken Gene Bank (Tsukuba, Japan), respectively. These cells were cultured in Dulbecco's modified Eagle's me-

TABLE 1

Sequence of oligonucleotides used in this study

Oligonucleotide	5′ to 3′ Sequence
For construction of cosmid DNA	
S-PGRMC1	GAGTTCCGGATCCCTGCC[a]
AS-PGRMC1	ATACCTCGAGAGATATACTTCCACTG[b]
S-CYP2E1-1	ATGTCTGCCCTCGGAGTCAC
AS-CYP2E1-1	CTCATGAGCGGGGAATGACA
For construction of FLAG-tagged PGRMC1 plasmid	
S-PGRMC1	See above sequence
AS-FLAG PGRMC1	TAGACTCGAG*CTA*CTTGTCATCGTCATCCTTGTAGTCATCATTTTTCCGGGCACTC[d]
For construction of Myc-tagged P450 plasmids	
S-CYP3A4	TCACTCGAGATGGCTCTCATCCCAGACTTG[b,c]
AS-CYP3A4	CTCGGTACC^GGCTCCACTTACGGTGCCATC[e]
S-CYP2C9	TCACTCGAGATGGATTCTCTTGTGGTC[b,c]
AS-CYP2C9	CTCGGTACC^GACAGGAATGAAGCACAGC[e]
S-CYP2E1-2	TCACTCGAGATGTCTGCCCTCGGAGTCAC[b,c]
AS-CYP2E1-2	CTCGGTACC^TGAGCGGGGAATGACACAGAG[e]
S-3×Myc	CTCGGTACCGAGCAGAAGCTGATCAGCGAGGAGGACCTGGAGCAGAAGCTGATCAGCG **AGGAGGACCTGGAGCAGAAGCTGATCAGCGAGGAGGACCTG*TGA*** GCGGCCGC GTCGACAG[f]
AS-3×Myc	CTGTCGACGCGGCCGC*TCA*CAGGTCCTCCTCGCTGATCAGCTTCTGCTCCAGGTCC **TCCTCGCTGATCAGCTTCTGCTCCAGGTCCTCCTCGCTGATCAGCTTCTGCTC** GGTACC GAG[g]

S, sense; AS, antisense.
[a] The BamHI site is underlined.
[b] The XhoI site is underlined.
[c] The start codon is in bold.
[d] The XhoI site is underlined. Complementary sequences of FLAG tag are in bold. Complementary sequences of stop codon (TAG) are italicized.
[e] The KpnI site is underlined. The deleted stop codon is shown with the inverted carat.
[f] The KpnI and NotI sites are underlined. Three tandem Myc tags are in bold. The stop codon (TGA) is italicized.
[g] The NotI and KpnI sites are underlined. Complementary sequences of three tandem Myc tags are in bold. Complementary sequences of stop codon (TGA) are italicized.

dium (Nissui, Tokyo, Japan) supplemented with 0.1 mM nonessential amino acid (Invitrogen) and 10% fetal bovine serum (Invitrogen). For the construction of the coexpression systems for FLAG-PGRMC1 and Myc-P450, the HEK293 cells were cultured in Dulbecco's modified Eagle's medium containing 4.5 g/l glucose, 10 mM HEPES, and 10% fetal bovine serum. Human cryopreserved hepatocytes, lot H704 (Caucasian, female, 49 years old), were purchased from XenoTech, LLC (Lenexa, KS). The hepatocytes were cultured in hepatocyte culture medium (HCM) (Cambrex, East Rutherford, NJ) on a plate coated with Cell Matrix Type I-C (Nitta Gelatin, Tokyo, Japan). These cells were maintained at 37°C under an atmosphere of 5% CO_2, 95% air.

Infection of Recombinant Adenoviruses to HepG2 Cells or Cryopreserved Human Hepatocytes. HepG2 cells were seeded at 7.5×10^5 cells/well into a six-well plate and were allowed to grow confluent. The cells were infected with a constant MOI of AdCYP (AdCYP3A4, 5; AdCYP2C9, 20; AdCYP2E1, 25; represented as ×1 in Fig. 1) and varied MOI of AdPGRMC1 (0, 2.5, 5, and 10 represented as 0, ×1, ×2, and ×4, respectively). To make the total MOI the same value in four different experimental conditions, AdGFP was infected. After 24 h, the cultured medium was replaced with fresh medium without adenovirus. After 48 h, total cell homogenates were prepared by homogenization with TGE buffer (10 mM Tris-HCl, pH 7.4, 20% glycerol, and 0.1 mM EDTA). The protein concentration was determined using Bradford protein assay reagent (Bio-Rad Laboratories, Hercules, CA) with γ-globulin as a standard.

The human hepatocytes were seeded at 1.5×10^6 cells/well into a 6-well plate. After 3 h, the medium was changed to HCM (albumin and antibiotics free) containing AdPGRMC1 or AdGFP at MOI 30. After 1 h, the medium was replaced with fresh HCM. After 48 h, the total cell homogenates were prepared as described above.

Human Liver Microsomes. Pooled human liver microsomes (HLMs) (n = 50) and individual HLMs (20 donors) were purchased from BD Gentest. Human liver samples from nine donors were obtained from the Human and Animal Bridging Research Organization (Chiba, Japan), which is in partnership with the National Disease Research Interchange (Philadelphia, PA). Microsomes were prepared according to the method described previously (Tabata et al., 2004).

SDS-Polyacrylamide Gel Electrophoresis and Western Blotting. Total cell homogenates or HLMs (20 μg) were separated with 10% SDS-polyacrylamide gel electrophoresis (PAGE) for the detection of P450s and with 15% SDS-PAGE for the detection of PGRMC1. The separated proteins were electrotransferred onto the polyvinylidene difluoride membrane Immobilon-P (Millipore). The membranes were probed with rabbit anti-human CYP3A4, goat anti-rat CYP2E1, rabbit anti-human CYP2C9, rabbit anti-human PGRMC1, anti-human/rat CPR, or anti-cytochrome b_5 antibodies and the corresponding fluorescent dye-conjugated secondary antibodies. The band densities were quantified with the Odyssey Infrared Imaging system (LI-COR Biosciences). The expression levels of P450 proteins were defined on the basis of a standard curve using P450 Supersomes (BD Gentest).

Enzyme Assays. A typical incubation mixture (final volume, 0.2 ml) contained 0.4 mg/ml total cell homogenate or 0.2 mg/ml HLM, 100 mM potassium phosphate buffer, pH 7.4, an NADPH-generating system (0.5 mM $NADP^+$, 5 mM glucose 6-phosphate, 5 mM $MgCl_2$, and 1 unit/ml glucose 6-phosphate dehydrogenase), and each substrate. The reaction mixture was preincubated at 37°C for 2 min, and the reaction was started by adding the NADPH-generating system.

The testosterone 6β-hydroxylase activity was determined as described previously (Nakajima et al., 1999) with a 20-min reaction time. The product formation was determined using HPLC with a LachromUltra C18 column (4.6 × 100 mm; 3 μm; Hitachi, Tokyo, Japan) and monitored at 240 nm.

The midazolam 1′-hydroxylase activity was determined as described previously (Kronbach et al., 1989) with slight modifications. The reaction mixture was incubated at 37°C for 15 min, and the reaction was terminated by adding 100 μl of ice-cold methanol. Clonazepam (20 ng) was added as an internal standard. After the removal of the protein by centrifugation at 10,000g for 5 min, a 20-μl portion of the sample was subjected to a liquid chromatography-tandem mass spectrometry system with an HP 1100 system including a binary pump, an automatic sampler, and a column oven (AB Sciex, Tokyo, Japan), which was equipped with a ZORBAX SB-C18 column (2.1 × 50 mm; 3.5 μm; Agilent Technologies). The column temperature was 20°C, and the flow rate was 0.2 ml/min. The mobile phase was 0.1% formic acid in water (A) and 0.1% formic acid in acetonitrile (B). A linear gradient was used from 20% B to 90% B over 2 to 3 min followed by 90% B for 7 min, and then the column was allowed to re-equilibrate at the initial conditions for 4 min. The liquid chromatography was connected to a PE Sciex API 2000 tandem mass spectrometer (AB Sciex) operated in the positive electrospray ionization mode. The turbo gas was maintained at 550°C. Nitrogen was used as the nebulizing gas, turbo gas, and curtain gas at 40, 90, and 40 psi, respectively. Parent and/or fragment ions were filtered in the first quadrupole and dissociated in the collision cell using nitrogen as the collision gas. The collision energy was 37 V. The mass/charge (m/z) ion transitions were recorded in the multiple reaction monitoring mode: m/z 342.0 and 203.0 for 1′-hydroxymidazolam; m/z 315.9 and 270.1 for clonazepam.

The S-warfarin 7-hydroxylase activity was determined as described previously (Yamazaki et al., 1997) with a 20-min incubation time. The product formation was determined using HPLC with a Mightysil RP-18 column (4.6 × 150 mm; 5 μm; Kanto Chemical, Tokyo, Japan) and monitored with the excitation wavelength set at 320 nm and the emission set at 415 nm.

The diclofenac 4′-hydroxylase activity was determined by the method used by Katoh et al. (2004) with a 30-min incubation time. The product formation was determined using HPLC with a TSK-GEL ODS-80T_M column (4.6 × 250 mm; 5 μm; TOSOH, Tokyo, Japan) and monitored at 280 nm.

The chlorzoxazone 6-hydroxylase activity was determined as described previously (Mohri et al., 2010) with a 30-min incubation time. The product formation was determined using HPLC with a LachromUltra C18 column (4.6 × 100 mm; 3 μm) and monitored at 295 nm.

The 7-ethoxycoumarin O-deethylase activity was determined as described previously (Yamazaki et al., 1999) with a 30-min incubation time. The product formation was determined using HPLC with a Mightysil RP-18 column (4.6 × 150 mm; 5 μm) and monitored with the excitation wavelength set at 338 nm and the emission set at 458 nm.

Kinetic parameters were estimated from the fitted curve using a computer program (KaleidaGraph; Synergy Software, Reading, PA) designed for nonlinear regression analysis. The following equations were used: Michaelis-Menten equation, $V = V_{max} \times [S]/(K_m + [S])$; and substrate inhibition equation, $V = V_{max} \times [S]/(K_m + S + [S]^2/K_i)$, where V is the velocity of the

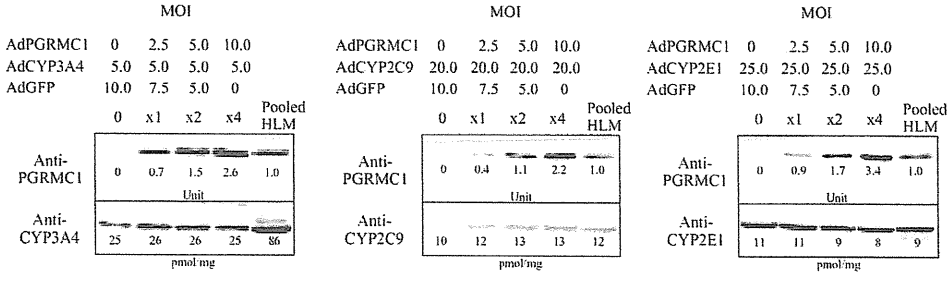

FIG. 1. Establishment of coexpression systems for PGRMC1 and CYP3A4, CYP2C9, or CYP2E1. HepG2 cells were infected with AdPGRMC1, each AdP450, and AdGFP for 72 h at the indicated MOI. Total MOI was adjusted by the infection of AdGFP. Twenty micrograms of total cell homogenates from the HepG2 or human liver microsomes were subjected to Western blot analyses. The absolute P450 protein levels were determined using a standard curve with each human P450 Supersome. The PGRMC1 protein levels were expressed relative to the value in the pooled HLMs set at 1.0. The values on the membrane are the mean of two independent determinations.

reaction, [S] is the substrate concentration, K_m is the Michaelis-Menten constant, V_{max} is the maximum velocity, and K_i is the substrate inhibition constant. Data are expressed as the means ± S.D. of three independent determinations.

Coimmunoprecipitation Assay. The FLAG-PGRMC1 and each Myc-P450 expression plasmid were transiently cotransfected into HEK293 cells. In brief, the day before transfection, the cells were seeded into a six-well plate coated with Cell Matrix Type I-C. After 24 h, each 2 μg of FLAG-PGRMC1 and Myc-P450 plasmids was transfected using Lipofectamine 2000. After 48 h, the cells were collected, and total cell homogenates were prepared by homogenization with TGE buffer. Five hundred micrograms of protein were suspended in either buffer A or buffer B in a final volume of 0.5 ml and rotated at 4°C for 2 h. Buffer A consisted of 0.5% Nonidet P-40, 0.25% sodium deoxycholate, 50 mM Tris-HCl, pH 7.4, 150 mM NaCl, 1 mM EDTA, 0.5 mM (*p*-amidinophenyl)-methanesulfonyl fluoride hydrochloride, 2 μg/ml aprotinin, and 2 μg/ml leupeptin. The detergents in buffer A were replaced with 0.1% digitonin in buffer B. The lysates were centrifuged at 100,000*g* for 30 min. To the supernatants, the anti-FLAG antibody was added and incubated for 8 h followed by precipitation with protein G-Sepharose beads. The beads were washed with buffer A or B and suspended with Laemmli sample buffer. The eluent was subjected to Western blot analyses with anti-FLAG antibody or anti-c-Myc antibody.

Statistical Analyses. Statistical significance was determined by using an unpaired, two-tailed Student's *t* test for paired data between two groups or the Shirley-Williams' test when more than three groups were compared. Correlation analyses were performed by Pearson's product-moment method. When the *P* value was less than 0.05, the differences were considered statistically significant.

Results

Establishment of Coexpression Systems for PGRMC1 and P450s in HepG2 Cells. To establish coexpression systems for PGRMC1 and P450s, AdPGRMC1 was cotransfected with AdCYP3A4, AdCYP2C9, or AdCYP2E1 into the HepG2 cells. Preliminarily, we optimized the MOIs to obtain the expression levels of PGRMC1 and P450s that are close to those in pooled human liver microsomes. When AdPGRMC1 was infected at MOI 3 to 4, the expressed PGRMC1 levels were close to those in the pooled HLMs. Accordingly, we set the MOIs for AdPGRMC1 at 2.5, 5, and 10, which were represented as ×1, ×2, and ×4, respectively (Fig. 1). The MOIs for AdCYP2C9 and AdCYP2E1 were set at 20 and 25, respectively. In the case of AdCYP3A4, MOIs over 10 showed cellular toxicity. Therefore, we set the MOIs for AdCYP3A4 at 5, although the level of CYP3A4 protein produced was lower than that in the pooled HLMs (Fig. 1) but was in the range of those in individual HLMs, as described below. Thus, we obtained four lines for each P450 with various levels of PGRMC1. Using these systems, we investigated the effects of PGRMC1 on the P450 activities.

Effects of Coexpression of PGRMC1 on CYP3A4 Activities. To investigate the effects of PGRMC1 on the CYP3A4 activity, kinetic analyses of testosterone 6β-hydroxylation and midazolam 1′-hydroxylation were performed using the total cell homogenates from the HepG2 coexpression system. The kinetics of testosterone 6β-hydroxylation followed the Michaelis-Menten equation (Fig. 2A). The K_m, V_{max}, and V_{max}/K_m values of the homogenates from the cells with no exogenous PGRMC1 were 56.9 ± 9.1 μM, 54.3 ± 4.0 pmol · min^{-1} · pmol $P450^{-1}$, and 0.96 ± 0.08 μl · min^{-1} · pmol $P450^{-1}$, respectively (Table 2). The coexpression of PGRMC1 significantly decreased the V_{max} values and increased the K_m values, resulting in a decrease in the V_{max}/K_m values in a PGRMC1 concentration-dependent manner. The kinetics of midazolam 1′-hydroxylation followed the substrate-inhibition equation (Fig. 2B). The K_m, V_{max}, K_i, and V_{max}/K_m values by the homogenates from the cells with no exogenous PGRMC1 were 5.7 ± 0.9 μM, 9.8 ± 1.5 pmol · min^{-1} · pmol $P450^{-1}$, 15.9 ± 4.1 μM, and 1.72 ± 0.03 μl · min^{-1} · $pmol^{-1}$ P450, respectively (Table 2). The coexpression of PGRMC1 significantly decreased the V_{max} values and increased the K_m values, resulting in a decrease in the V_{max}/K_m values in a PGRMC1 concentration-dependent manner. The K_i value was not affected by the coexpression of PGRMC1. Thus, it was demonstrated that PGRMC1 has the ability to attenuate the CYP3A4 activity independently of the substrate.

Effects of Coexpression of PGRMC1 on CYP2C9 Activities. To investigate the effects of PGRMC1 on the CYP2C9 activity, kinetic analyses of *S*-warfarin 7-hydroxylation and diclofenac 4′-hydroxylation were performed. The kinetics of *S*-warfarin 7-hydroxylation followed the Michaelis-Menten equation (Fig. 3A). The K_m, V_{max}, and V_{max}/K_m values by the homogenates from the cells with no exogenous PGRMC1 were 1.6 ± 0.1 μM, 5.4 ± 0.2 pmol · min^{-1} · pmol $P450^{-1}$, and 3.3 ± 0.2 μl · min^{-1} · pmol $P450^{-1}$, respectively (Table 3). The coexpression of PGRMC1 significantly decreased the V_{max} values in a PGRMC1 concentration-dependent manner but did not affect the K_m values, resulting in a decrease in the V_{max}/K_m values. The kinetics of diclofenac 4′-hydroxylation followed the Michaelis-Menten equation (Fig. 3B). The K_m, V_{max}, and V_{max}/K_m values by the homogenates from the cells with no exogenous PGRMC1 were 7.3 ± 0.3 μM, 91.6 ± 6.8 pmol · min^{-1} · pmol $P450^{-1}$, and 12.6 ± 1.5 μl · min^{-1} · pmol $P450^{-1}$, respectively (Table 3). The coexpression of PGRMC1

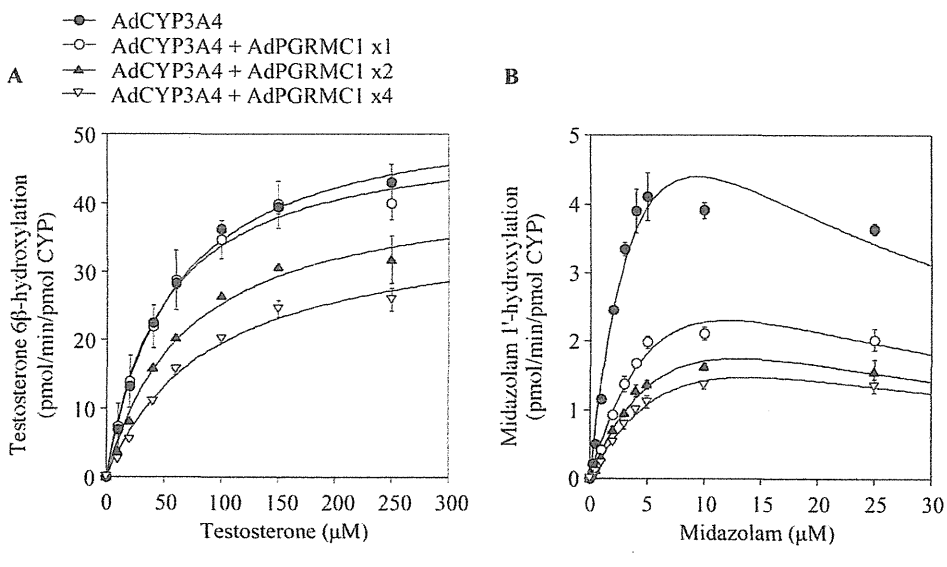

FIG. 2. Kinetic analyses of testosterone 6β-hydroxylation (A) and midazolam 1′-hydroxylation (B) by recombinant CYP3A4 in single or coexpression systems with PGRMC1. The expression systems were constructed using recombinant adenoviruses as described under *Materials and Methods*. The obtained kinetic parameters are shown in Table 2. Data are the means ± S.D. of three independent determinations.

TABLE 2

Kinetic parameters for testosterone 6β-hydroxylase activity and midazolam 1′-hydroxylase activity by recombinant CYP3A4 in single or coexpression systems with PGRMC1

The expression systems were constructed using recombinant adenoviruses as described under *Materials and Methods*. Kinetic parameters were calculated from curves by nonlinear regression. Data are mean ± S.D. of three independent experiments.

AdCYP3A4 + AdPGRMC1	Testosterone 6β-Hydroxylation			Midazolam 1′-Hydroxylation			
	K_m	V_{max}	V_{max}/K_m	K_m	V_{max}	K_i	V_{max}/K_m
	μM	*pmol · min^{-1} · pmol P450^{-1}*	*μl · min^{-1} · pmol P450^{-1}*	*μM*	*pmol · min^{-1} · pmol P450^{-1}*	*μM*	*μl · min^{-1} · pmol P450^{-1}*
	56.9 ± 9.1	54.3 ± 4.0	0.96 ± 0.08	5.7 ± 0.9	9.8 ± 1.5	15.9 ± 4.1	1.72 ± 0.03
×1	53.1 ± 22.3	51.2 ± 5.9	1.07 ± 0.42	10.9 ± 2.2*	6.5 ± 0.7*	10.4 ± 7.5	0.60 ± 0.05*
×2	71.4 ± 14.2	43.4 ± 4.4*	0.62 ± 0.07*	11.6 ± 3.8*	5.0 ± 1.4*	17.8 ± 11.6	0.44 ± 0.04*
×4	91.8 ± 12.2*	37.4 ± 2.7**	0.41 ± 0.04*	12.5 ± 2.1*	4.1 ± 0.6**	16.3 ± 3.1	0.33 ± 0.01**

* $P < 0.05$ and ** $P < 0.01$ compared with control by Shirley-Williams' test.

significantly decreased the V_{max} values in a PGRMC1 concentration-dependent manner but did not affect the K_m values, resulting in a decrease in the V_{max}/K_m values. Thus, it was demonstrated that PGRMC1 has the ability to attenuate the CYP2C9 activity independently of the substrate.

Effects of Coexpression of PGRMC1 on CYP2E1 Activities. To investigate the effects of PGRMC1 on the CYP2E1 activity, kinetic analyses of chlorzoxazone 6-hydroxylation and 7-ethoxycoumarin O-deethylation were performed. The kinetics of chlorzoxazone 6-hydroxylation followed the Michaelis-Menten equation (Fig. 4A). The K_m, V_{max}, and V_{max}/K_m values by the homogenates from the cells with no exogenous PGRMC1 were 67.1 ± 5.6 μM, 618.3 ± 18.2 pmol · min^{-1} · pmol P450^{-1}, and 9.3 ± 0.5 μl · min^{-1} · pmol P450^{-1}, respectively (Table 4). The coexpression of PGRMC1 did not affect the kinetic parameters. The kinetics of 7-ethoxycoumarin O-deethylation followed the Michaelis-Menten equation (Fig. 4B). The K_m, V_{max}, and V_{max}/K_m values by the homogenates from the cells with no exogenous PGRMC1 were 40.2 ± 2.5 μM, 16.0 ± 1.2 pmol · min^{-1} · pmol P450^{-1}, and 0.40 ± 0.01 μl · min^{-1} · pmol P450^{-1}, respectively (Table 4). The coexpression of PGRMC1 did not affect the K_m and V_{max} values but slightly decreased the V_{max}/K_m values. PGRMC1 likely had a small effect on the CYP2E1 activities in comparison with the CYP3A4 and CYP2C9.

Effects of Overexpression of PGRMC1 on Enzyme Activities in Human Hepatocytes. To investigate whether PGRMC1 modulates the activities of endogenous human P450s, we sought to overexpress PGRMC1 in human hepatocytes. When the homogenates from the human hepatocytes were subjected to Western blot analysis, the band density of PGRMC1 protein was similar to that in the pooled HLMs (Fig. 5A). When AdPGRMC1 was infected, the PGRMC1 protein level was significantly (5.6-fold, $P < 0.001$) increased (Fig. 5A). We confirmed that there was no morphological change by the infection with AdPGRMC1. Using the homogenates from these cells, the midazolam 1′-hydroxylase, *S*-warfarin 7-hydroxylase, and chlorzoxazone 6-hydroxylase activities, at the substrate concentrations of 10, 10, and 500 μM, respectively, were evaluated. Interestingly, we found that the midazolam 1′-hydroxylase and *S*-warfarin 7-hydrozylase activities in the homogenates from the AdPGRMC1-infected cells were significantly lower than those in control (AdGFP-infected cells). In contrast, the chlorzoxazone 6-hydroxylase activity was not affected by the overexpression of PGRMC1 (Fig. 5B). These results suggest that PGRMC1 modulates the endogenous human P450 activity in an isoform-specific manner, supporting the results from the expression systems.

Coimmunoprecipitation of PGRMC1 and P450s. To investigate whether PGRMC1 directly interacts with P450s, we used a coimmunoprecipitation assay. Because commercially available antibodies against PGRMC1 or P450s are not suitable for immunoprecipitation assays, we constructed FLAG-PGRMC1 and Myc-P450 coexpression systems to perform the immunoprecipitation assay using anti-tag antibodies. We confirmed, by Western blot analyses using anti-FLAG and anti-c-Myc antibodies, that both FLAG-PGRMC1 and Myc-P450s were successfully expressed (Fig. 6). When the lysates using buffer A were assayed, the PGRMC1 in the three expression systems

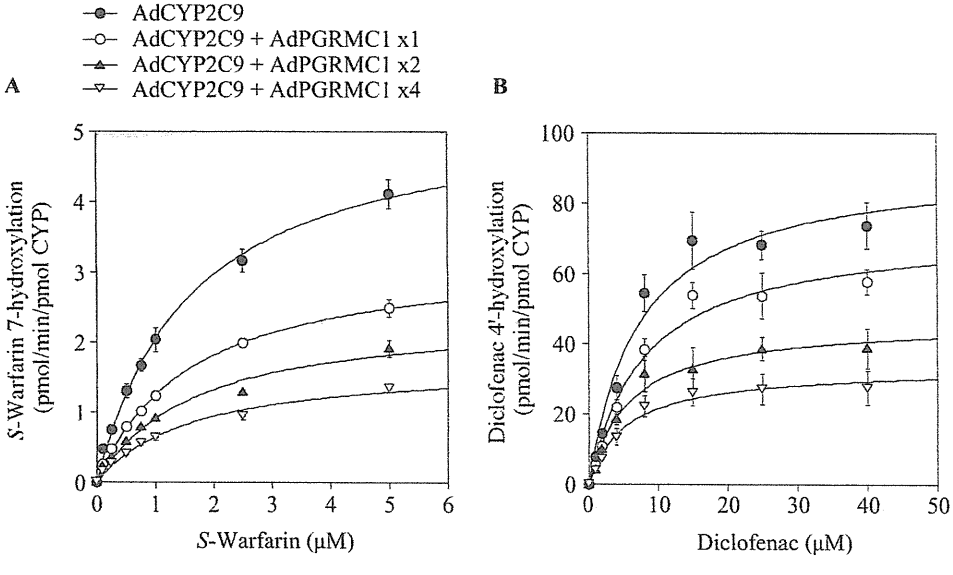

FIG. 3. Kinetic analyses of *S*-warfarin 7-hydroxylation (A) and diclofenac 4′-hydroxylation (B) by recombinant CYP2C9 in single or coexpression systems with PGRMC1. The expression systems were constructed using recombinant adenoviruses as described under *Materials and Methods*. The obtained kinetic parameters are shown in Table 3. Data are the means ± S.D. of three independent determinations.

TABLE 3

Kinetic parameters for S-warfarin 7-hydroxylase activity and diclofenac 4′-hydroxylase activity by recombinant CYP2C9 in single or coexpression systems with PGRMC1

The expression systems were constructed using recombinant adenoviruses as described under *Materials and Methods*. Kinetic parameters were calculated from curves by nonlinear regression. Data are mean ± S.D. of three independent experiments.

	S-Warfarin 7-Hydroxylation			Diclofenac 4′-Hydroxylation		
AdCYP2C9 + AdPGRMC1	K_m	V_{max}	V_{max}/K_m	K_m	V_{max}	V_{max}/K_m
	μM	$pmol \cdot min^{-1} \cdot pmol\ P450^{-1}$	$\mu l \cdot min^{-1} \cdot pmol\ P450^{-1}$	μM	$pmol \cdot min^{-1} \cdot pmol\ P450^{-1}$	$\mu l \cdot min^{-1} \cdot pmol\ P450^{-1}$
	1.6 ± 0.1	5.4 ± 0.2	3.3 ± 0.2	7.3 ± 0.3	91.6 ± 6.8	12.6 ± 1.5
×1	1.6 ± 0.1	3.3 ± 0.2*	2.0 ± 0.1*	8.1 ± 0.5	72.9 ± 4.7*	9.0 ± 0.5*
×2	1.7 ± 0.2	2.4 ± 0.2**	1.5 ± 0.1**	7.1 ± 2.7	52.5 ± 15.5**	7.5 ± 0.5**
×4	1.7 ± 0.2	1.7 ± 0.1**	1.0 ± 0.1**	8.4 ± 0.6	42.2 ± 6.7**	5.0 ± 0.5**

* $P < 0.05$ and ** $P < 0.01$ compared with control by Shirley-Williams' test.

was immunoprecipitated to the same extent by using the anti-FLAG antibody, and only Myc-CYP2E1 was coimmunoprecipitated (Fig. 6A). When the lysates using buffer B were assayed, all three P450s were coimmunoprecipitated (Fig. 6B). These results suggest that PGRMC1 binds directly to these P450s, although the degree would be different among the isoforms.

Relationship between P450 Activities and PGRMC1, CPR, and Cytochrome b_5 Levels in a Panel of 29 Human Liver Microsomes. The midazolam 1′-hydroxylase, *S*-warfarin 7-hydroxylase, and chlorzoxazone 6-hydroxylase activities in a panel of 29 human liver microsomes were measured at the substrate concentrations of 10, 5, and 500 μM, and the PGRMC1, CYP3A4, CYP2C9, CYP2E1, CPR, and cytochrome b_5 protein levels were determined by Western blot analysis. The variability of the PGRMC1 protein levels was ~5-fold (Table 5). Although the variability of the CYP3A4 protein levels was large (3–72 pmol/mg, 24-fold), those of the CYP2C9 (5–17 pmol/mg, ~3-fold) and the CYP2E1 (3–16 pmol/mg, ~5-fold) protein levels were relatively small. As shown in Supplemental Fig. 1, A–C, the midazolam 1′-hydroxylase, *S*-warfarin 7-hydroxylase, and chlorzoxazone 6-hydroxylase activities represented as the metabolite $\cdot\ min^{-1} \cdot$ mg $protein^{-1}$ were significantly correlated with CYP3A4, CYP2C9, and CYP2E1, respectively. To investigate whether the PGRMC1 would be a factor modulating the P450 activities, correlation analyses between the ratio of PGRMC1 to P450 and the midazolam 1′-hydroxylase, *S*-warfarin 7-hydroxylase, and chlorzoxazone 6-hydroxylase activities represented as the metabolite $min^{-1} \cdot$ pmol $P450^{-1}$ were performed. We expected inverse correlations between PGRMC1/CYP3A4 ratio and midazolam 1′-hydroxylase or PGRMC1/CYP2C9 ratio and *S*-warfarin 7-hydroxylase activities based on the results of the coexpression systems in HepG2 cells. However, no inverse correlation was observed (Supplemental Fig. 1, D–F). In addition, except for the CPR/CYP2E1 ratio, the CPR/P450 or cytochrome b_5/P450 ratios did not show a positive correlation with the activities (Supplemental Fig. 1, G–L). Next, we determined the relationship between the PGRMC1 protein level, and each P450 activity corrected with the CPR protein (Supplemental Fig. 2, A–C) or cytochrome b_5 protein (Supplemental Fig. 2, D–F) levels. However, no inverse correlation was observed in the CYP3A4 or CYP2C9 activities. Because the PGRMC1 protein levels were significantly correlated with the CPR ($r = 0.50$, $P < 0.01$) and cytochrome b_5 ($r = 0.76$, $P < 0.0001$) protein levels (Supplemental Fig. 2, G and H), it would be difficult to estimate the contribution of PGRMC1 to the P450 activities in HLM by the correlation analyses.

Discussion

In this study, we investigated the effects of PGRMC1 on the human drug-metabolizing P450 activities, focusing on three major isoforms, CYP3A4, CYP2C9, and CYP2E1. Using coexpression systems for PGRMC1/P450s in HepG2 cells, we found that PGRMC1 increased the K_m and decreased the V_{max} of the CYP3A4 activities and decreased the V_{max} of the CYP2C9 activities irrespective of the substrates (Figs. 2 and 3). In contrast to CYP3A4 and CYP2C9, PGRMC1 did not dramatically affect the CYP2E1 activities, indicating the effects of PGRMC1 would be P450 isoform dependent. During the process of preparing this report, an independent study reported that PGRMC1 commonly decreased the CYP3A4, CYP2C8, and rabbit

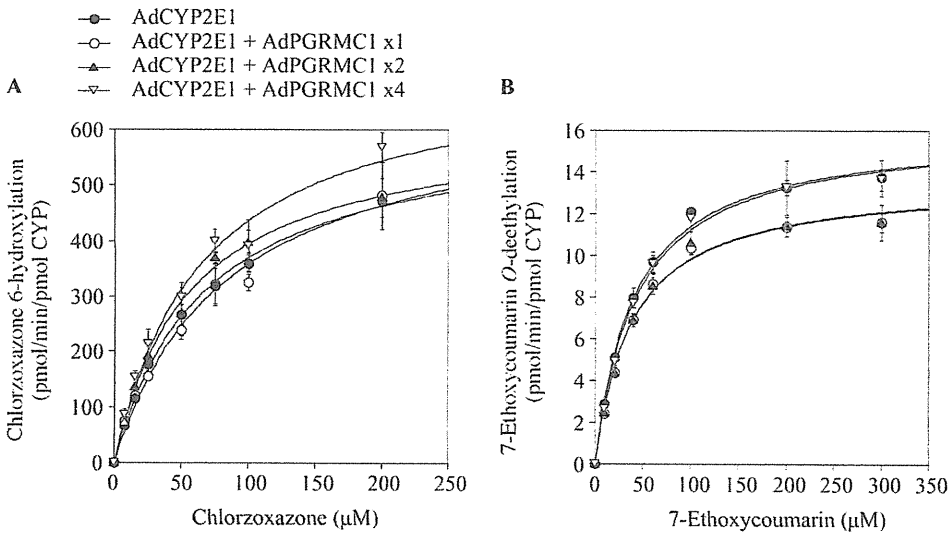

FIG. 4. Kinetic analyses of chlorzoxazone 6-hydroxylation (A) and 7-ethoxycoumarin O-deethylation (B) by recombinant CYP2E1 in single or coexpression systems with PGRMC1. The expression systems were constructed using recombinant adenoviruses as described under *Materials and Methods*. The obtained kinetic parameters are shown in Table 4. Data are the means ± S.D. of three independent determinations.

TABLE 4

Kinetic parameters for chlorzoxazone 6-hydroxylase activity and 7-ethoxycoumarin O-deethylase activity by recombinant CYP2E1 in single or coexpression systems with PGRMC1

The expression systems were constructed using recombinant adenoviruses as described under *Materials and Methods*. Kinetic parameters are calculated from curves by nonlinear regression. Data are mean ± S.D. of three independent experiments.

	Chlorzoxazone 6-Hydroxylation			7-Ethoxycoumarin O-Deethylation		
AdCYP2E1 + AdPGRMC1	K_m	V_{max}	V_{max}/K_m	K_m	V_{max}	V_{max}/K_m
	μM	$pmol \cdot min^{-1} \cdot pmol\ P450^{-1}$	$\mu l \cdot min^{-1} \cdot pmol\ P450^{-1}$	μM	$pmol \cdot min^{-1} \cdot pmol\ P450^{-1}$	$\mu l \cdot min^{-1} \cdot pmol\ P450^{-1}$
	67.1 ± 5.6	618.3 ± 18.2	9.3 ± 0.5	40.2 ± 2.5	16.0 ± 1.2	0.40 ± 0.01
×1	85.5 ± 21.6	667.8 ± 112.7	8.0 ± 0.8	38.3 ± 0.6	13.6 ± 0.4	0.35 ± 0.02*
×2	56.1 ± 8.2	617.9 ± 56.1	11.1 ± 0.6	38.3 ± 0.8	13.6 ± 0.7	0.36 ± 0.01*
×4	65.6 ± 7.2	723.1 ± 52.6	11.1 ± 1.0	42.6 ± 1.5	16.0 ± 0.4	0.38 ± 0.02*

* $P < 0.05$ compared with control by Shirley-Williams' test.

CYP2C2 activities using coexpression systems in HEK293 cells (Szczesna-Skorupa and Kemper, 2011). They evaluated the enzyme activities by P450-Glo assay at a substrate concentration. The findings that PGRMC1 decreased the activities of drug-metabolizing P450s were similar between our and recent reports, but our new findings are that the effects of PGRMC1 on the kinetics were different between the P450 isoforms and that there exists a P450(s) not affected by PGRMC1. When we mixed the homogenates from the single expression system for PGRMC1 and the homogenates from the single expression system for P450s, no changes were observed in the kinetics of each P450 activity (data not shown). Therefore, it was suggested that colocalization on the membrane would be critical for PGRMC1 to exert its effect in modulating the P450 activities. It has been reported that PGRMC1 is predominantly located in the endoplasmic reticulum. However, in a human ovarian cancer cell line, Ovcar-3, PGRMC1 is found in the cytoplasm (Lösel et al., 2008). To analyze the localization of PGRMC1 in human liver, we performed Western blot analysis using cytosol, but PGRMC1 could not be detected. Therefore, the subcellular localization of PGRMC1 appears to be cell-type specific.

To investigate whether PGRMC1 modulates the activities of endogenous P450, we performed experiments using human hepatocytes. First, we sought to investigate the effects of repression of PGRMC1 by siRNA on the P450 activities (data not shown). When siRNA for PGRMC1 (Stealth select RNAi; Invitrogen) was transfected into human hepatocytes, the PGRMC1 mRNA levels were decreased by 70%. However, the PGRMC1 protein level was not decreased (data not shown). Although we used additional siRNA for PGRMC1 from another supplier (Ambion, Austin, TX), favorable results were not obtained. Hence, we sought to investigate the effects of the overexpression of PGRMC1 in human hepatocytes. The overexpression of PGRMC1 resulted in decreases in the CYP3A4 and CYP2C9 activities, but not CYP2E1 activity, which were the same as with the HepG2 coexpression systems (Fig. 5). These results suggest that PGRMC1 modulates the activities of endogenous P450 in an isoform-specific manner.

Using the coimmunoprecipitation assay (Fig. 6), we found that PGRMC1 interacts with P450s (not only CYP3A4 and CYP2C9 but also CYP2E1). When buffer A containing Nonidet P-40 and sodium deoxycholate, which are relatively strong detergents, was used, only CYP2E1 was coimmunoprecipitated (Fig. 6A). However, when buffer B containing digitonin, which is a relatively weaker detergent, was used, all of the three P450 isoforms were coimmunoprecipitated (Fig. 6B). These results suggested that the binding of PGRMC1 to CYP2E1 might be stronger than the binding to CYP3A4 or CYP2C9. Alternatively, the number of CYP2E1 molecules that bound to a PGRMC1 molecule might be larger than that of CYP3A4 or CYP2C9. In other words, a smaller number of PGRMC1 molecules may bind to CYP2E1. Such differences might explain why PGRMC1 did not affect the CYP2E1 activity but decreased the CYP3A4 and CYP2C9 activities, or the effects of PGRMC1 might not be a simple protein-protein interaction.

It was demonstrated that introduction of a mutation in the cytochrome b_5-like domain of PGRMC1, to which heme binds, abolishes the binding to CYP7A1 (Mansouri et al., 2008). Min et al. (2005) also reported that a heme-deficient PGRMC1 mutant could not increase the CYP21A2 activity. These observations suggest the importance of heme binding for PGRMC1 in its function. Cytochrome b_5 has a hexacoordinate heme that is capable of transferring an electron. Mean-

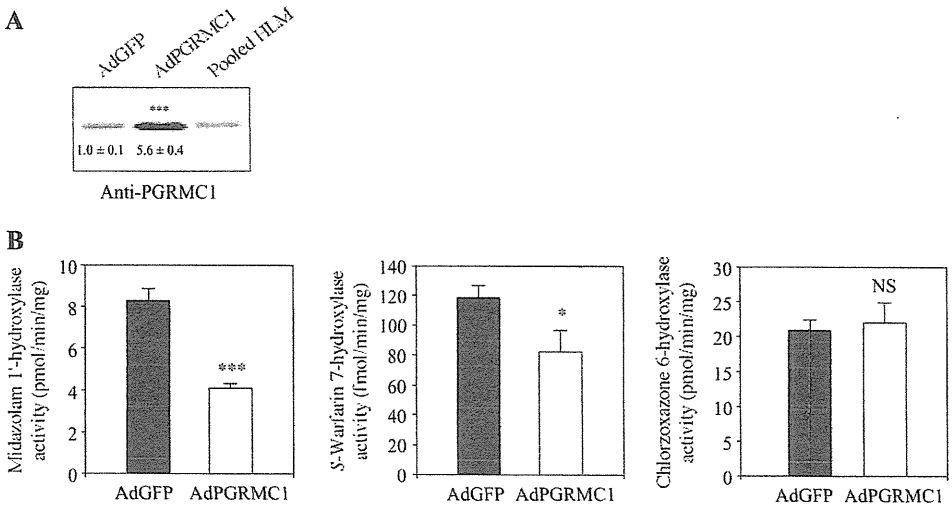

FIG. 5. Effects of overexpression of PGRMC1 on P450 activities in human hepatocytes. Human hepatocytes were infected with Ad-PGRMC1 or AdGFP at MOI 30. After 48 h, cells were collected and total cell homogenates were prepared. A, expression level of PGRMC1 in the homogenates (10 μg) was determined by Western blot analysis. Pooled HLMs (20 μg) were also subjected. B, midazolam 1'-hydroxylase activity (at 10 μM substrate concentration), *S*-warfarin 7-hydroxylase activity (at 10 μM substrate concentration), and chlorzoxazone 6-hydroxylase activity (at 500 μM substrate concentration) in the homogenates were measured. *, $P < 0.05$; ***, $P < 0.001$. NS, not significant.

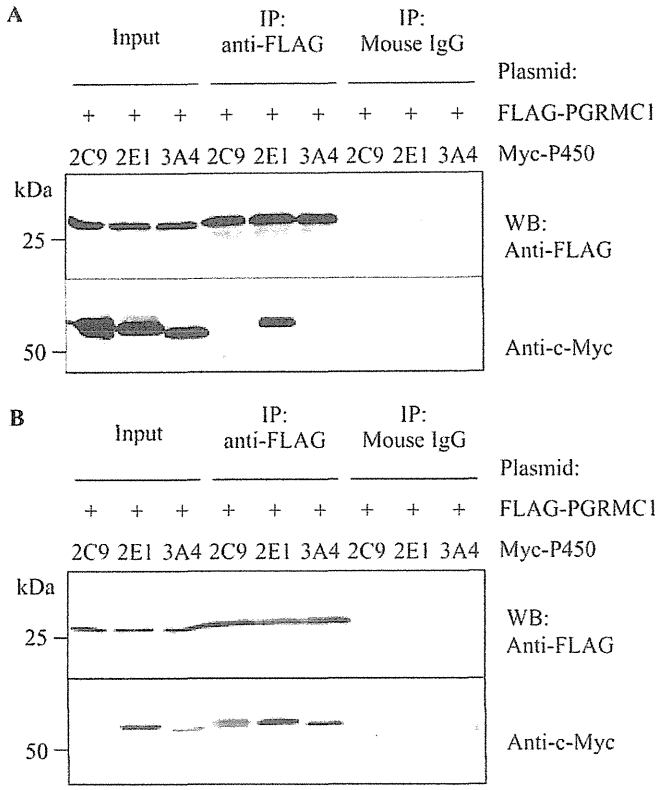

FIG. 6. Coimmunoprecipitation of FLAG-PGRMC1 and Myc-P450. FLAG-PGRMC1 plasmid and Myc-P450 (CYP3A4, CYP2C9, and CYP2E1) plasmid were transiently cotransfected into HEK293 cells. Five hundred micrograms of protein of the total cell homogenates were solubilized with buffer A (A) or buffer B (B) and immunoprecipitated with anti-FLAG antibody. The immunoprecipitates were subjected to SDS-PAGE followed by Western blot analyses using the anti-FLAG antibody or anti-Myc antibody. Input proteins (20 μg) were also subjected to Western blot. Data are representative of at least three independent experiments. IP, immunoprecipitation; WB, Western blot.

while, PGRMC1 has a pentacoordinate heme (Cahill, 2007; Rohe et al., 2009), suggesting that PGRMC1 does not donate electrons to P450. Therefore, PGRMC1 affects the P450 function without direct electron transfer. Szczesna-Skorupa and Kemper (2011) reported that the PGRMC1-dependent inhibition of P450 activities is partially restored by the overexpression of CPR. In addition, because the coimmunoprecipitation of CPR and PGRMC1 was observed, they concluded that PGRMC1 binds to CPR and decreases the P450 activities. In contrast to their study, the coimmunoprecipitation of CPR and PGRMC1 was not observed in our system using HEK293 cells without the overexpression of CPR, probably because of the low expression level (data not shown). Alternatively, we measured the cytochrome *c* reduction and found that PGRMC1 did not alter the CPR activity (Supplemental Table 1). Thus, the decrease in the P450 activities by PGRMC1 might not be due to the decrease in CPR activity, although the possibility that PGRMC1 might influence the electron transferring from CPR to P450, because the V_{max} values of CYP3A4 and CYP2C9 were decreased, could not be excluded. In the case of CYP3A4, an increase in the K_m values was also observed. Therefore, as another mechanism, it is suggested that PGRMC1 might cause an allosteric change in the CYP3A4 structure that affects the affinity to substrates. Nevertheless, the effects of PGRMC1 on the P450 activity were diverse depending on the P450 isoforms, and further detailed studies are needed to clarify the underlying mechanisms.

In this study, the variability of the PGRMC1 protein levels in HLM was first evaluated. In 29 human liver samples, there was 5-fold variability (Table 5). We sought to estimate the contribution of PGRMC1 to the modulation of the P450 activities by correlation analyses between the P450 activities and P450 or PGRMC1 protein levels. In the analysis, we took into account the other components, the transferring of electrons to P450 such as CPR or cytochrome b_5. Although these components positively regulate the enzyme activities of CYP3A4, CYP2C9, and CYP2E1, no clear correlation with the P450 activities was observed except in the case of CYP2E1. It has been reported that the molar ratio of P450/CPR/cytochrome b_5 seems to be important to understanding the role of CPR in the modulation of the P450 activities. We can determine the absolute expression levels of P450, CPR, and cytochrome b_5 but not PGRMC1. Understanding the absolute expression level of PGRMC1 in HLMs would be helpful to determine the relative importance of PGRMC1 in the modulation of the P450 activity.

Previous studies reported that PGRMC1 increased the activities of CYP21A2 and CYP51A1 that are responsible for steroid or sterol metabolism (Min et al., 2005; Hughes et al., 2007). In contrast, this study found that PGRMC1 decreased the activity of human drug-metabolizing P450s, which is supported in the study by Szczesna-Skorupa and Kemper (2011), although it is possibly isoform dependent. It has been reported that PGRMC1 is highly expressed in breast and ovary tumors and in cancer cell lines from the colon, thyroid, lung, and cervix (Crudden et al., 2005; Peluso et al., 2008a). Recently, it has been reported that PGRMC1 is highly expressed in human myometrium during pregnancy and may mediate the relaxation effect on myometrium (Wu et al., 2011). The changes of PGRMC1 expression under certain physiological conditions might impact on the metabolism of steroids. Meanwhile, little is known about the factors that affect the PGRMC1 expression level in human liver. Further studies are warranted to clarify the physiological significance of PGRMC1 in the modulation of drug-metabolizing P450 in liver.

In conclusion, we found that PGRMC1 decreases the activities of drug-metabolizing P450s in an isoform-dependent manner. The action was opposite to that for steroid-metabolizing P450s. Thus, PGRMC1 seems to affect P450s depending on their functions. The present study

TABLE 5

Expression levels of PGRMC1, P450s, CPR, and cytochrome b_5 and enzyme activities in human liver microsomes

Mean ± S.D. and range of each value from 29 individual human liver microsomes are shown. Data are the mean of duplicate determinations.

	Relative Expression Level			Expression Level			Enzyme Activity		
	PGRMC1[a]	CPR[b]	Cyt b_5[b]	CYP3A4	CYP2C9	CYP2E1	MDZ	*S*-War	CZX
					pmol/mg		*nmol · min^{-1} · mg^{-1}*	*pmol · min^{-1} · mg^{-1}*	*nmol · min^{-1} · mg^{-1}*
Mean ± S.D.	0.62 ± 0.25	1.9 ± 0.3	2.8 ± 1.4	28 ± 20	9 ± 3	9 ± 4	2.4 ± 2.1	2.1 ± 1.3	1.6 ± 0.7
Range	0.23–1.23	1.0–2.6	1.0–6.3	3–72	5–17	3–16	0.1–8.5	0.5–5.6	0.7–3.6

Cyt b_5, cytochrome b_5; MDZ, midazolam 1′-hydroxylase activity; *S*-war, *S*-warfarin 7-hydroxylase activity; CZX, chlorzoxazone 6-hydroxylase activity.
[a] PGRMC1 protein level was expressed as relative to the pooled HLMs set at 1.0.
[b] CPR and cytochrome b_5 protein levels are indicated as relative to the lowest set at 1.0.

revealed a novel function of PGRMC1 in modulating the drug-metabolizing activity.

Acknowledgments

We acknowledge Brent Bell for reviewing this manuscript.

Authorship Contributions

Participated in research design: Oda, Nakajima, Fukami, and Yokoi.

Conducted experiments: Oda.

Contributed new reagents or analytic tools: Oda, Toyoda, and Fukami.

Performed data analysis: Oda and Nakajima.

Wrote or contributed to the writing of the manuscript: Oda, Nakajima, and Yokoi.

References

Cahill MA (2007) Progesterone receptor membrane component 1: an integrative review. *J Steroid Biochem Mol Biol* **105:**16–36.

Crudden G, Loesel R, and Craven RJ (2005) Overexpression of the cytochrome p450 activator hpr6 (heme-1 domain protein/human progesterone receptor) in tumors. *Tumour Biol* **26:**142–146.

Debose-Boyd RA (2007) A helping hand for cytochrome p450 enzymes. *Cell Metab* **5:**81–83.

Ghosh K, Thompson AM, Goldbeck RA, Shi X, Whitman S, Oh E, Zhiwu Z, Vulpe C, and Holman TR (2005) Spectroscopic and biochemical characterization of heme binding to yeast Dap1p and mouse PGRMC1p. *Biochemistry* **44:**16729–16736.

Guengerich FP (2002) Rate-limiting steps in cytochrome P450 catalysis. *Biol Chem* **383:**1553–1564.

Hosomi H, Akai S, Minami K, Yoshikawa Y, Fukami T, Nakajima M, and Yokoi T (2010) An in vitro drug-induced hepatotoxicity screening system using CYP3A4-expressing and γ-glutamylcysteine synthetase knockdown cells. *Toxicol In Vitro* **24:**1032–1038.

Hughes AL, Powell DW, Bard M, Eckstein J, Barbuch R, Link AJ, and Espenshade PJ (2007) Dap1/PGRMC1 binds and regulates cytochrome P450 enzymes. *Cell Metab* **5:**143–149.

Iwamura A, Fukami T, Hosomi H, Nakajima M, and Yokoi T (2011) CYP2C9-mediated metabolic activation of losartan detected by a highly sensitive cell-based screening assay. *Drug Metab Dispos* **39:**838–846.

Katoh M, Matsui T, Nakajima M, Tateno C, Kataoka M, Soeno Y, Horie T, Iwasaki K, Yoshizato K, and Yokoi T (2004) Expression of human cytochromes P450 in chimeric mice with humanized liver. *Drug Metab Dispos* **32:**1402–1410.

Kronbach T, Mathys D, Umeno M, Gonzalez FJ, and Meyer UA (1989) Oxidation of midazolam and triazolam by human liver cytochrome P450IIIA4. *Mol Pharmacol* **36:**89–96.

Laird SM, Vinson GP, and Whitehouse BJ (1988) Monoclonal antibodies against rat adrenocortical cell antigens. *Acta Endocrinol (Copenh)* **119:**420–426.

Locuson CW, Gannett PM, and Tracy TS (2006) Heteroactivator effects on the coupling and spin state equilibrium of CYP2C9. *Arch Biochem Biophys* **449:**115–129.

Lösel RM, Besong D, Peluso JJ, and Wehling M (2008) Progesterone receptor membrane component 1—many tasks for a versatile protein. *Steroids* **73:**929–934.

Mansouri MR, Schuster J, Badhai J, Stattin EL, Lösel R, Wehling M, Carlsson B, Hovatta O, Karlström PO, Golovleva I, et al. (2008) Alterations in the expression, structure and function of progesterone receptor membrane component-1 (PGRMC1) in premature ovarian failure. *Hum Mol Genet* **17:**3776–3783.

Mifsud W and Bateman A (2002) Membrane-bound progesterone receptors contain a cytochrome b_5-like ligand-binding domain. *Genome Biol* **3:**RESEARCH0068.

Min L, Takemori H, Nonaka Y, Katoh Y, Doi J, Horike N, Osamu H, Raza FS, Vinson GP, and Okamoto M (2004) Characterization of the adrenal-specific antigen IZA (inner zone antigen) and its role in the steroidogenesis. *Mol Cell Endocrinol* **215:**143–148.

Min L, Strushkevich NV, Harnastai IN, Iwamoto H, Gilep AA, Takemori H, Usanov SA, Nonaka Y, Hori H, Vinson GP, et al. (2005) Molecular identification of adrenal inner zone antigen as a heme-binding protein. *FEBS J* **272:**5832–5843.

Mohri T, Nakajima M, Fukami T, Takamiya M, Aoki Y, and Yokoi T (2010) Human CYP2E1 is regulated by miR-378. *Biochem Pharmacol* **79:**1045–1052.

Nakajima M, Nakamura S, Tokudome S, Shimada N, Yamazaki H, and Yokoi T (1999) Azelastine N-demethylation by cytochrome P-450 (CYP)3A4, CYP2D6, and CYP1A2 in human liver microsomes: evaluation of approach to predict the contribution of multiple CYPs. *Drug Metab Dispos* **27:**1381–1391.

Nebert DW and Russell DW (2002) Clinical importance of the cytochromes P450. *Lancet* **360:**1155–1162.

Nelson DR, Zeldin DC, Hoffman SM, Maltais LJ, Wain HM, and Nebert DW (2004) Comparison of cytochrome P450 (CYP) genes from the mouse and human genomes, including nomenclature recommendations for genes, pseudogenes and alternative-splice variants. *Pharmacogenetics* **14:**1–18.

Peluso JJ, Liu X, Saunders MM, Claffey KP, and Phoenix K (2008a) Regulation of ovarian cancer cell viability and sensitivity to cisplatin by progesterone receptor membrane component-1. *J Clin Endocrinol Metab* **93:**1592–1599.

Peluso JJ, Romak J, and Liu X (2008b) Progesterone receptor membrane component-1 (PGRMC1) is the mediator of progesterone's antiapoptotic action in spontaneously immortalized granulosa cells as revealed by PGRMC1 small interfering ribonucleic acid treatment and functional analysis of PGRMC1 mutations. *Endocrinology* **149:**534–543.

Rohe HJ, Ahmed IS, Twist KE, and Craven RJ (2009) PGRMC1 (progesterone receptor membrane component 1): a targetable protein with multiple functions in steroid signaling, P450 activation and drug binding. *Pharmacol Ther* **121:**14–19.

Shimada T, Yamazaki H, Mimura M, Inui Y, and Guengerich FP (1994) Interindividual variations in human liver cytochrome P-450 enzymes involved in the oxidation of drugs, carcinogens and toxic chemicals: studies with liver microsomes of 30 Japanese and 30 Caucasians. *J Pharmacol Exp Ther* **270:**414–423.

Szczesna-Skorupa E and Kemper B (2011) Progesterone receptor membrane component 1 inhibits the activity of drug-metabolizing cytochromes P450 and binds to cytochrome P450 reductase. *Mol Pharmacol* **79:**340–350.

Tabata T, Katoh M, Tokudome S, Hosakawa M, Chiba K, Nakajima M, and Yokoi T (2004) Bioactivation of capecitabine in human liver: involvement of the cytosolic enzyme on 5'-deoxy-5-fluorocytidine formation. *Drug Metab Dispos* **32:**762–767.

Wu W, Shi SQ, Huang HJ, Balducci J, and Garfield RE (2011) Changes in PGRMC1, a potential progesterone receptor, in human myometrium during pregnancy and labour at term and preterm. *Mol Hum Reprod* **17:**233–242.

Yamazaki H, Gillam EM, Dong MS, Johnson WW, Guengerich FP, and Shimada T (1997) Reconstitution of recombinant cytochrome P450 2C10(2C9) and comparison with cytochrome P450 3A4 and other forms: effects of cytochrome P450–P450 and cytochrome P450-b_5 interactions. *Arch Biochem Biophys* **342:**329–337.

Yamazaki H, Tanaka M, and Shimada T (1999) Highly sensitive high-performance liquid chromatographic assay for coumarin 7-hydroxylation and 7-ethoxycoumarin O-deethylation by human liver cytochrome P450 enzymes. *J Chromatogr B Biomed Sci Appl* **721:**13–19.

Address correspondence to: Dr. Tsuyoshi Yokoi, Drug Metabolism and Toxicology, Faculty of Pharmaceutical Sciences, Kanazawa University, Kakuma-machi, Kanazawa 920-1192, Japan. E-mail: tyokoi@kenroku.kanazawa-u.ac.jp